We would like to thank the reviewers for their valuable comments and suggestions. We have considered all comments carefully which helped us significantly to improve our manuscript. Following the reviewers' comments and suggestions, we revised the manuscript. Our responses to the reviewers' comments are listed below in blue fonts and the changes in manuscript are listed in *blue italic fonts*.

Anonymous Referee #1

Received and published: 21 March 2019

This manuscript presents continuous measurements of PBL structure using a newly developed compact lidar system combined both direct detection lidar and coherent Doppler win lidar, and demonstrates that the PBL height can be accurately retreated by the measurements and the residual BL and stable BL can be distinguished using different signals from the instrument. The relationships between the PM2.5 concentration and the PBL height were also analyzed. The authors found a strong negative correlation between PM2.5 and PBL height before the precipitation event and a much weaker negative correlation after the precipitation.

The manuscript is well organized and written in general. The instrument is demonstrated as very useful in boundary layer research. The quality of the observations is very impressive. The results and analyses are clear and persuasive. Some of the conclusions need to be rephrased under certain contexts. After the following points are addressed, the manuscript is recommended to be published on AMT.

Thanks for your positive comments. We have rewritten some conclusions in the revised manuscript.

1. Page 1, line 17. Suggest removing "Negative".

Corrected as suggested.

Changes: Page 1, line 18-19. "*Correlation between different BLH and $PM_{2.5}$ is strongly negative before a precipitation event and become much weaker after the precipitation*."

2. It is not an ideal location for the weather site to be on the top of a building. The building impacts the temperature, humidity, wind speed and direction. Cautions should be used when analyzing the weather data from such a site.

Thanks for this comment. In fact, there is not any ideal location for the weather site in such an urban area. The overly dense buildings will also impact the temperature, humidity, wind speed and direction on the ground. We will pay attention to these cautions when analyzing these data.

Changes: Page 6, line 33 - page 7, line 1. "*It should be noted that the building where the instrument deployed would have an impact on these meteorological parameters.*"

3. Page 4, line 22. The variance of vertical velocity should just represent the vertical component of the turbulent kinetic energy.

Corrected as suggested.

Changes: Page 5, line 10-11. "*The BLH can also be determined from the variance of vertical velocity σ_w^2, which represents the vertical component of the turbulence kinetic energy*."

4. Page 5. Model-simulated PBL height in a relatively coarse grid spacing cannot be used to cross-check the observation even though the reanalysis data have assimilated lots of observations. Sounding is probably a better source for observation cross-check. I would recommend the authors to show the 12-hourly sounding data in the city and compare them with the lidar observed PBL structure.

Thanks for this suggestion. Unfortunately, there is not any sounding data in Hefei. The nearest sounding station is in Anqing, which is approximately 150 km south to Hefei. A cross-check of BLH retrieved from lidar and sounding data will be carried out in future experiments or observations.

Changes: Page 5, line 22-23. "*The hourly BLH from high resolution realisation sub-daily deterministic forecasts of ERA5 is used to cross-check the BLH retrieved from lidar since there is no sounding data in Hefei.*"

5. Page 6. How strong was the precipitation event? The authors are recommended to provide quantified value of the precipitation either from the met station observation or model-based estimate. The strength of the precipitation impacts the PM2.5 concentration after the event. Usually strong rainfall will scavenge most of the PM2.5 particles while drizzle or light rain can moisten the PBL and facilitate wet growth of smaller aerosols that reach PM2.5.

Thanks for your valuable suggestion. There is no precipitation event as drizzle or light rain recorded by the weather transmitter (Vaisala WXT520) or experimenter on the ground or the top of the building. As you suggested, such precipitation event as drizzles above the ground may increase the aerosol, which consists our observation.

Changes: Page 7, line 1-2. "*There is no precipitation event recorded on the ground by weather transmitter, even during the precipitation in the cloud as shown in Fig. 3c.*"

6. Page 7, line 32. As mentioned in previous comment, there may not be unknown sources but just the wet growth of the existing small particles.

Thanks for this suggestion. The relationships between BLH and $PM_{2.5}$ are affected after the precipitation. The wet growth of small particles may be responsible during the drizzles. However, during the growing process of CBL after the precipitation, the correlation between BLH and $PM_{2.5}$ is weak even after the drizzles as shown in Fig. 5e and Table 2. This weak relationship when there is no drizzle can't be explained by wet growth of aerosols. Thus, both the pollution sources and meteorological conditions should be considered. We modified this description and added some discussions in the revised manuscript.

Changes:

Page 7, line 10-11. "*The wet growth of the existing small particles caused by the precipitation above the ground may be responsible for the sudden increase of aerosols.*"

Page 8, line 23-24. "*The relationships between BLH and PM2.5 are changed after precipitation.*"

7. Page 14, figure 3. I would recommend the authors to identify RL and SBL tops and if possible, together with the RL bottom at the same time based on the data. These fine structures are extremely useful for model validation and parameterization development.

Thanks for this suggestion. We identified RL top as red dotted lines with a temporal resolution of 5 min in revised Fig. 3. The dominant aerosol layer top is retrieved based on threshold method. If the difference between aerosol layer top and BLH is larger than a specified threshold, 0.3 km in current study, the aerosol layer is identified as the RL top. For the SBL top and RL bottom, it is difficult to be identified due to elevated aerosol layers, e.g., between 1 June 2018 21:00 and 2 June 2018 03:00. For the turbulence derived SBL, the vertical resolution (60 m) of the lidar used in this study is too coarse for an accuracy SBL near the ground (< 200 m). We have developed a new lidar recently, which has higher spatial resolution of meter-scale to solve this problem in future work (Wang et al., 2019). Therefore, we only identified RL tops in the revised manuscript.

Changes:

Page 5, line 29-30. "*Compared to the BLH retrieval, RL top can be identified through a simply rough threshold which is described in the Appendix.*"

Page 10, line 5-15. "***Appendix: The RL top retrieval method***

Besides BLH, RL top is also important in model validation and parameterization development. A simple method to retrieve RL top from RCS, CNR and variance of vertical velocity profiles is proposed. In order to reduce the interference from noise, the RL top is determined with a temporal resolution of 5 min. Dominant aerosol layer tops are easy to be identified around 2 km altitude as shown in Fig, 3. Thus the aerosol layer tops are limited between 1 and 2.5 km altitude range. A threshold method is suitable for RCS and CNR profiles. For this observation, the threshold is set to be 5×10^{10} *for RCS profile (*1×10^{10} *for resolution of 1 min as shown in Fig. 3a) and -30 dB for CNR profile. For profiles of variance of vertical velocity, the aerosol layer is identified as the altitudes under the minimum altitude where invalid data exists, e.g., ~1.6 km in Fig. 2c. If the difference between aerosol layer top and BLH is larger than a threshold, e.g., 0.3 km in current study, the aerosol layer top is identified as RL top. It should be noted that all the values of threshold used here may varies at different places for different lidars. These values may be only suitable for during this observation.*"

8. Page 16, figure 5e. These relationships are indeed the result of both cloud effect and precipitation impacts not just precipitation causing the differences. A modeling study is needed to untangle these two effects and quantify the contributions to the changes of the relationships.

Thanks for this comment. This is a good suggestion to probe the different effects by using a model. The reasons for the differences in the relationships may result from both cloud effect and pollutant sources not just precipitations. This study is focus on the relationship between $PM_{2.5}$ and BLH based on a hybrid lidar, not the mechanism of the differences in the relationships. More observational and modeling study are needed to solve this question in future work.

Changes:

Page 8, line 23-28. "*The relationships between BLH and PM2.5 are changed after precipitation. Recently, Geiß et al. (2017) investigated correlations between BLH and concentrations of pollutants (PM_{10}, O_3, NO_x). They found that the correlations of BLH with PM_{10} were quite different for different sites without showing a clear pattern. In addition, the reflection and absorption of the incoming solar radiation by the clouds on 2 June 2018 could also affect the diffusion of aerosols. Therefore, BLH with different retrieval methods, pollutant sources and meteorological conditions should be considered in air quality prediction models.*"

Page 9, line 23-24. "*The reasons for the differences in the relationships between BLH and $PM_{2.5}$ may result from both cloud effect and pollutant sources not just the precipitation*."

Page 9, line 26-27. "*To probe the mechanism of the BLH-$PM_{2.5}$ relations under different conditions, such as before and after the precipitation, not only such observations, but also model simulation are needed in further studies.*"

Anonymous Referee #3

Received and published: 28 April 2019

The manuscript aims to investigate the relationship between BLH and air pollution in different ABL categories. The ABLH is defined based on both a micro-pulse lidar (DDL) and a coherent Doppler wind lidar (CDWL) through wavelet covariance transform method and variance analysis of the vertical velocity. It is well written and the analysis is careful. However, there are some aspects for improvement:

Thanks for your careful and thoughtful comments. We revised the manuscript according to your suggestions.

1. Only the relationship between PM2.5 and BLH before and after one precipitation process is analyzed. The manuscript only presents the phenomena, so what accounts for this difference, what role of the precipitation process, it is unclear;

The precipitation event above the ground may be responsible for the sudden increase of aerosol due to wet growth of smaller aerosols. The precipitation may lead to this difference in the early hours after the precipitation. *Geiß et al.*, 2017 investigated the relashionship between BLH and PM_{10}. They found that the pollution sources, meteorological conditions and BLH retrieval details should be considered. In addition, the cloud effect should also be considered. Thus a complex process which is unknown accounts for this difference. More observations in under different conditions and modeling study would be helpful to improve our knowledge on this complex topic.

Changes:

Page 8, line 23-28. "*The relationships between BLH and PM2.5 are changed after precipitation. Recently, Geiß et al. (2017) investigated correlations between BLH and concentrations of pollutants (PM_{10}, O_3, NO_x). They found that the correlations of BLH with PM_{10} were quite different for different sites without showing a clear pattern. In addition, the reflection and absorption of the incoming solar radiation by the clouds on 2 June 2018 could also affect the diffusion of aerosols. Therefore, BLH with different retrieval methods, pollutant sources and meteorological conditions should be considered in air quality prediction models.*"

Page 9, line 23-24. "*The reasons for the differences in the relationships between BLH and $PM_{2.5}$ may result from both cloud effect and pollutant sources not just the precipitation*."

Page 9, line 26-27. "*To probe the mechanism of the BLH-$PM_{2.5}$ relations under different conditions, such as before and after the precipitation, not only such observations, but also model simulation are needed in further studies.*"

2. ABL may not belong to different categories before and after the precipitation, in fact, according to the Figure 3(a), the growing process of the CBL after the precipitation is very similar to that before the precipitation;

Yes, the growing processes of the CBL before and after the precipitation are similar. In Sect. 4.3, we mentioned that "*In general, these results show good responses of $PM_{2.5}$ to aerosol derived BLH (BLH_{RCS}) evolution with larger R^2 and stronger correlation than turbulence derived BLH (BLH_{VAR}) both before and after precipitation*." The different ABL categories in this manuscript mean that aerosol derived BLH (static, i.e., BLH_{RCS} and BLH_{CNR}) and turbulence derived BLH (dynamical, i.e., BLH_{VAR}). We are very sorry for this confusing expression and modified it in the revised manuscript.

Changes: Page 8, line 16-18. "*In general, these results show good responses of $PM_{2.5}$ to aerosol derived BLH (BLH_{RCS}) evolution with larger R^2 and stronger correlation than turbulence derived BLH (BLH_{VAR}) both before and after precipitation*."

3. From your manuscript, anti-correlation relationship between PM2.5 and BLH is found whether before or after a precipitation. The difference is that the relativity weakened after a precipitation. It seems that precipitation plays an important role. That is, the author paid more attention to different weather conditions instead of "different ABL categories ".

Thanks for this comment. As answered to comment 2, the different ABL categories are ABL retrieved from aerosol signal and turbulence, respectively. We have discussed the different relationships between $PM_{2.5}$ and BLH under different ABL categories (BLH_{RCS} and BLH_{VAR}) in Sect.4.3 and Table 2. We apologize for this confusing expression in the manuscript.

Changes:

Page 2, line 16-18. "*However, the relationship analysis of $PM_{2.5}$ and BLH in different ABL categories, i.e., aerosol derived (static) BLH and turbulence derived (dynamical) BLH, is still rare*."

Page 8, line 16-18. "*In general, these results show good responses of $PM_{2.5}$ to aerosol derived BLH (BLH_{RCS}) evolution with larger R^2 and stronger correlation than turbulence derived BLH (BLH_{VAR}) both before and after precipitation*."

4. The core content of the manuscripts is the "Relationship Analysis of PM2.5 and BLH", from the abstract, only the sentence "Negative correlation between BLH and PM2.5 is analyzed before and after a precipitation." is related to your title. And such conclusion is very common, lower concentration of PM always corresponds to higher BLH if there is no new emission source. The abstract does not show the purpose and innovation point of the study explicitly. Besides, only one paragraph describes the relationship of PM2.5 and BLH in the text? The abstract and the contents of the manuscripts should be improved.

Thanks for your comment. We revised the title as "Relationship Analysis of $PM_{2.5}$ and BLH using an Aerosol and Turbulence Detection Lidar". The relationship analysis is based on this innovative hybrid lidar. The advantages of this hybrid

lidar is introduced in responses to minor comment 4 and 6. Then, the BLH retrieval method and retrieved BLH results should be evaluated. Finally, the relationship analysis can be performed. Thus, all of these are related to the title, not only one paragraph. In previous work, the correlation could be negative, but also positive (*Geiß et al.*, 2017). So comparing the correlation under different conditions and places in the world is desired to improve our understanding of this complex topic: relashionship between PM and BLH. The relashionship analysis before and after precipitation in this study may be helpful to this complex topic. We also revised the abstract and the contents according to your suggestions.

Changes:

Page 1, line 1-2. "*Relationship Analysis of $PM_{2.5}$ and BLH using an Aerosol and Turbulence Detection Lidar*"

Page 1, line 18-20. "*Correlation between different BLH and $PM_{2.5}$ is strongly negative before a precipitation event and become much weaker after the precipitation. Different relations between $PM_{2.5}$ and BLH may result from different BLH retrieval methods, pollutant sources and meteorological conditions*."

Page 8, line 23-28. "*The relationships between BLH and PM2.5 are changed after precipitation. Recently, Geiß et al. (2017) investigated correlations between BLH and concentrations of pollutants (PM_{10}, O_3, NO_x). They found that the correlations of BLH with PM_{10} were quite different for different sites without showing a clear pattern. In addition, the reflection and absorption of the incoming solar radiation by the clouds on 2 June 2018 could also affect the diffusion of aerosols. Therefore, BLH with different retrieval methods, pollutant sources and meteorological conditions should be considered in air quality prediction models*."

Page 9, line 23-24. "*The reasons for the differences in the relationships between BLH and $PM_{2.5}$ may result from both cloud effect and pollutant sources not just the precipitation*."

Page 9, line 26-27. "*To probe the mechanism of the BLH-$PM_{2.5}$ relations under different conditions, such as before and after the precipitation, not only such observations, but also model simulation are needed in further studies.*"

Some minor revisions are as follows:

1. For line 3 on page 2, "The boundary layer height (BLH) is the height of the top layer of ABL", the description makes no sense, please improve.

Deleted.

2. For line 9 on page 2: Explain "ABL categories" here.

Thanks for this comment. The ABL categories are explained in the revised manuscript. "*different ABL categories, i.e., aerosol derived (static) BLH and turbulence derived (dynamical) BLH*"

Changes: Page 2, line 16-18. "*However, the relationship analysis of $PM_{2.5}$ and BLH in different ABL categories, i.e., aerosol derived (static) BLH and turbulence derived (dynamical) BLH, is still rare*."

3. For line 18 on page 2, “Among these instruments, lidar provides sufficient spatial and temporal resolution, long detection range and high accuracy to determine the BLH……”, the description should be improved, lidar system provides backscattering signal with sufficient spatial and temporal
resolution……

Corrected as suggested.

Changes: Page 2, line 16-18. “*Among these instruments, lidar system provides backscattering signal with sufficient spatial and temporal resolution, long detection range and high accuracy to determine the BLH.*”

4. For Lines 20-27 on page 2: Here, please highlight the advantages of two lidars.

Thanks for this suggestion. We added some advantages of these two lidars.

Changes:

Page 2, line 25-26. “*Recently, a micro-pulse direct detection lidar (DDL) based on up-conversion technology was developed to make continuous measurements of aerosol in troposphere (Xia et al., 2015)*”

Page 2, line 27-32. “*Different from traditional micro-pulse lidars operated at or near 532 nm (He et al., 2008; Li et al., 2017b; Sawyer and Li, 2013), these two lidars are operated at 1.5 μm, which are eye-safe and can be made with all-fiber components. The 1.5 μm laser shows the highest maximum permissible exposure in the wavelength range from 0.3 to 10 μm (Xia et al., 2015). The invisible infrared eye-safe laser makes these two lidars can work in a densely populated city horizontally. The all-fiber structure makes these lidars robust, immune to external environment changes such as vibration and temperature.*”

5. For lines 22-24 on page 2, “in middle atmosphere via Rayleigh scattering……, in mesosphere and lower thermosphere via fluorescence backscatter…….” The manuscripts focused on ABL, it may be unnecessary to mention the detection principle in middle atmosphere and in mesosphere and lower thermosphere.

Deleted as suggested.

6. For lines 25-26 on page 2, “Recently, a micro-pulse direct detection lidar (DDL) was developed to make continuous measurements of aerosol in troposphere…..” In fact, the micro-pulse lidar (MPL) has been widely used to detect ABLH, there are several studies (He et al., 2008; Sawyer and Li 2013; Li et al., 2017), not recently, maybe you can describe the advantage of the MPL here, such as detecting with eye-safe laser, small field-of-view removing multiple-layer scattering concerns……
As well as for description about Doppler wind lidar later.

He Q, Li C, Mao J, et al. Analysis of aerosol vertical distribution and variability in Hong Kong [J]. Journal of Geophysical Research Atmospheres, 2008, 113(D14):-.

Sawyer, V.; Li, Z.J.A.E.; Detection, variations and intercomparison of the planetary boundary layer depth from radiosonde, lidar and infrared spectrometer. 2013, 79 (11), 518-528.

Li, H.; Yang, Y.; Hu, X.M.; Huang, Z.; Wang, G.; Zhang, B.J.A.; Application of Convective condensation Level Limiter in Convective Boundary Layer Height Retrieval Based on Lidar Data. 2017, 8 (4), 79

Thanks for this suggestion. The micro-pulse direct detection lidar (DDL) is "*based on up-conversion technology*". "*Different from traditional micro-pulse lidars operated at or near 532 nm (He et al., 2008; Li et al., 2017b; Sawyer and Li, 2013), these two lidars are operated at 1.5 μm, which are eye-safe and can be made with all-fiber components. The 1.5 μm laser shows the highest maximum permissible exposure in the wavelength range from 0.3 to 10 μm (Xia et al., 2015). The invisible infrared eye-safe laser makes these two lidars can work in a densely populated city horizontally. The all-fiber structure makes these lidars robust, immune to external environment changes such as vibration and temperature*." Then the two lidars are integrated into one lidar system. "*In this work, a hybrid lidar integrating both systems are developed for simultaneous measurements of aerosol and vertical wind*." The advantages of this hybrid lidar has been described in Sect. 2.1. "*Two lidar systems use only one set of laser source, optical collimator and control system. The unique optical telescope guarantees that the measured signal in both systems are from the same backscattering volume, and the radial wind profile and aerosol concentration are measured simultaneously.*" We also showed the advantages of this hybrid lidar in the abstract and conclusions in the revised manuscript.

Changes:

Page 1, line 12-13. "*This hybrid lidar is operated at 1.5 μm which is eye-safe and is made of all-fiber components*."

Page 2, line 25-26. "*Recently, a micro-pulse direct detection lidar (DDL) based on up-conversion technology was developed to make continuous measurements of aerosol in troposphere (Xia et al., 2015)*"

Page 2, line 27-32. "*Different from traditional micro-pulse lidars operated at or near 532 nm (He et al., 2008; Li et al., 2017b; Sawyer and Li, 2013), these two lidars are operated at 1.5 μm, which are eye-safe and can be made with all-fiber components. The 1.5 μm laser shows the highest maximum permissible exposure in the wavelength range from 0.3 to 10 μm (Xia et al., 2015). The invisible infrared eye-safe laser makes these two lidars can work in a densely populated city horizontally. The all-fiber structure makes these lidars robust, immune to external environment changes such as vibration and temperature.*"

Page 9, line 8-11. "*The DDL incorporated a fiber laser at 1.5 μm and an up-conversion detector. This design of lidar makes it more eye-safe than traditional laser of 355, 532 and 1064 nm. All-fiber configuration is realized to guarantee the high optical coupling efficiency and robust stability. Two lidar systems use only one set of laser source, optical collimator and control system.*"

7. For lines 15-16 on page 4, "Considering different vertical spatial resolutions, a dilation of 150 m and 250 m is applied for RCS and CNR, respectively". The selection of an appropriate dilation is the key for WCT method. So why "150 m" and "250 m" are selected? Should be explained.

Thanks for this suggestion. We fully agree with your point of view "The selection of an appropriate dilation is the key for WCT method". Too large or too small dilation is not appropriate. We have tested different values of dilation as shown in Fig. R1, even height-dependent dilation that selected by previous studies for WCT method. At least for this 45 hour observations

from 1 June to 2 June in Hefei, 150 m is one of the most appropriate values of dilation for RCS. The 250 m for CNR is similar. In fact, the optimum value is equal to the depth of the transition zone (Brooks, 2003). The depth of transition zone varies in different places and seasons. A further study of transition zone depth is desirable by multi instruments with longer enough observations.

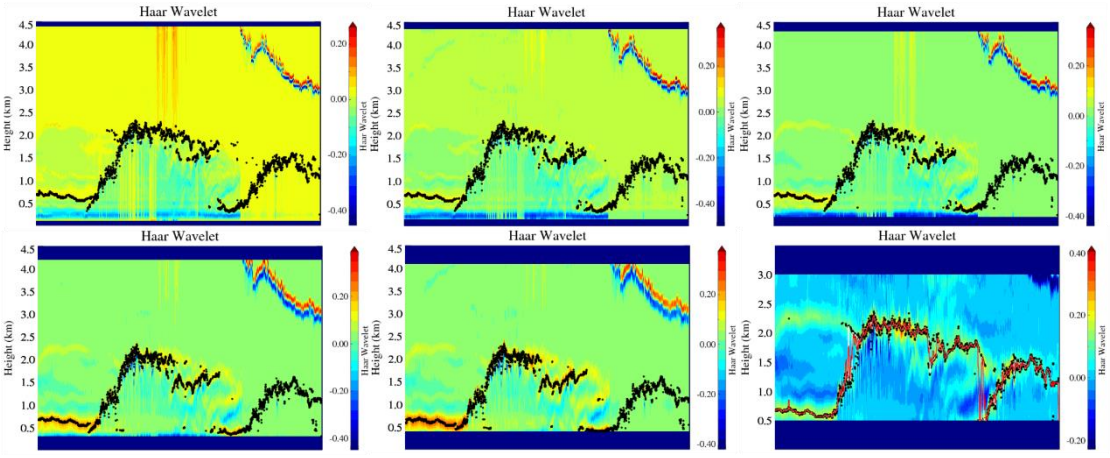

Figure R1. WCT method with different values of dilation for RCS. The values of dilation are 100 m, 150 m and 200 m for upper panels, 300 m, 400 m and 500 m for bottom panels, from left to right. The colored contours indicate the WCT results. The black dotted lines indicate retrieved BLH.

Changes: Page 4, line 21-22. "*Considering different vertical spatial resolutions and having tested multi values of dilation, a dilation of 150 m and 250 m is applied for RCS and CNR, respectively for this 45-hour observations*."

8. For line 16 on page 4, "Compared with gradient method, HWCT method has greater adjustability and robustness". In fact, as extended technique of gradient method, several studies (Brooks, 2003; Mao et al., 2013; Dang et al., 2019) have indicated the WCT method is also easily interference by multiple aerosol layers or cloud layer. So how the paper ideals with the interference of the cloud layers on ABLH determination in Figure 3(a)-(b)? No doubt, the signal gradient at the cloud boundary is strongest than at the ABL top on 2 June 2018, the HWCT may capture the cloud top rather than the true height of lower stable ABL.

Brooks, I.M.J.J.o.A.; Technology, O.; Finding Boundary Layer Top: Application of Wavelet covariance Transform to Lidar Backscatter Profiles. 2003, 20 (8), 1092—1105.

Mao, F.; Wei, G.; Song, S.; Zhu, Z.; Determination of the boundary layer top from lidar backscatter profiles using a Haar wavelet method over Wuhan, China. Optics Laser Technology 2013, 49 (7), 343-349.

Dang, R.; Yang, Y.; Li, H.; Hu, X.-M.; Wang, Z.; Huang, Z.; Zhou, T.; Zhang, T.; Atmosphere Boundary Layer Height (ABLH) Determination under Multiple-Layer Conditions Using Micro-Pulse Lidar. remote sensing 2019, 11 (263).

Thanks for this comment. For the cloud layer and aerosol layer higher than 2.5 km as shown in Fig. 3, we can easily remove the interference of such cloud layers above ABL by setting a top-limit of the WCT method in this manuscript similar

to Dang et al., 2019. For the multiple aerosol layers in the ABL, an appropriate dilation is useful and robust as shown in Fig. R1. For the scattered stratocumulus that exist in the capping layer as shown in Fig. 3a and 3b, the difference between cloud top and BLH are relatively small. In addition, the duration time of stratocumulus is also short in the field of view of the lidar that can be easily removed by a longer temporal resolution. Thus the influence of scattered stratocumulus is negligible. For the continuous thick low level cloud not shown in this observation, the BLH cannot be retrieved. Thus, the interference of the cloud layers and multiple aerosol layers are negligible at least in this manuscript. We added some description of the cloud in Sect. 3 in the revised manuscript.

Changes: Page 5, line 1-6. "*It should be noted that cloud layer could affect the BLH results. A top-limit is set to the HWCT method for higher clouds. For the scattered stratocumulus that may exist in the capping layer, the differences between cloud top and BLH are relatively small. In addition, the duration time of stratocumulus is also short in the field of view of the lidar. Thus the influence of scattered stratocumulus is negligible. The low level cloud in the ABL can be identified by the paired minimum $W_f(a,b)$ and maximum $W_f(a,b)$ occurs at heights close to each other. The BLH cannot be retrieved under this condition.*"

9. For line 17 on page 4, "In order to reduce the interference from unexpected turbulence and noise", what is unexpected turbulence? Is the "turbulence" is ambiguous here? Similarly, line 25 on page 4.

Thanks for this comment. We removed "turbulence" here in line 17. But in line 25, the unexpected turbulence means turbulence occurs in the free atmosphere where no turbulence is considered to exists.

Changes:

Page 4, line 24 – page 5, line 1. "*In order to reduce the interference from unexpected noise, the signal is averaged to a temporal resolution of 1 min in BLH determination.*"

Page 5, line 13-14. "*A median algorithm is used to mitigate the interference and fluctuation from unexpected turbulence and noise in the free atmosphere*"

10. For lines 19-20 on page 4, "As an example, the measured RCS and CNR after one-minute average (after overlap correction and background noise deduction) at 1 June 2018, 10:40 am is shown in Fig. 2a", Figure 2 shows an example in clear sky situation, profiles in cloudy situations on 2 June 2008 is suggested.

Thanks for this suggestion. As answered to minor comment 8, the interference of the clouds is removed by setting a top-limit of 2.5 km in this manuscript. Besides, to propose a robust BLH retrieval method under complex conditions is beyond the scope of current manuscript, but such work is desirable with more observations in future.

Changes:

Page 5, line 2. "*A top-limit is set to the HWCT method for higher clouds.*"

Page 7, line 15. "*A top-limit of 2.5 km of BLH is applied during the BLH retrieval*."

11. For line 22 on page 4, "…which represented the turbulence kinetic energy", the "represented" should change to "represents".

Corrected as suggested.

Changes: Page 5, line 10-11. "*The BLH can also be determined from the variance of vertical velocity σ_w^2, which represents the vertical component of the turbulence kinetic energy*."

12. For line 24 on page 4, "In this study, the threshold is set to be 0.06 m2s-2", how the threshold is defined?

Similar to that of dilation, we have tested different values of threshold for this observation. The variance of vertical velocity with 5 min temporal resolution is shown in Fig. R2. A threshold between 0.04 m^2s^{-2} and 0.15 m^2s^{-2} may be appropriate. As shown in Fig. 2c, 0.06 m^2s^{-2} is one of the most appropriate threshold during this observation. A smaller value may be difficult to identify free atmosphere while a larger value may be difficult to distinguish CBL with several lower variances, such as the profiles shown in Fig. 2c. It should also be noted that the threshold may varies with different places and seasons.

Changes: Page 5, line 12-13. "*In this study, the threshold is set to be 0.06 m^2s^{-2} which is suitable as shown in Fig. 2c*."

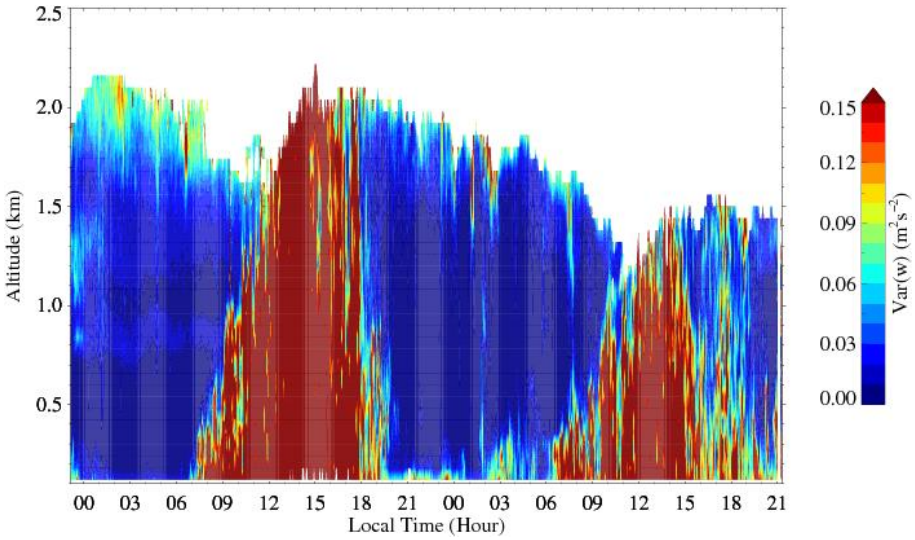

Figure R2. Variance of vertical velocity with 5 min temporal resolution.

13. For line 4 on page 5, "BLH from reanalysis data is always used in boundary layer climatology", please improve the description.

We modified this sentence as follows: "*Reanalysis data is always used in climatological and regional analysis of BLH (Collaud Coen et al., 2014; Guo et al., 2016; Seidel et al., 2012)*."

Changes: Page 5, line 18-19. "*Reanalysis data is always used in climatological and regional analysis of BLH (Collaud Coen et al., 2014; Guo et al., 2016; Seidel et al., 2012)*."

14. For lines 7-8 on page 5, "The hourly BLH from high resolution realization sub-daily deterministic forecasts of ERA5 is used here", is the ABLH defined from ERA used to estimate the results from lidar? The purpose should be stated. In addition, should "realisation" be changed to "realization"?

Yes, the hourly BLH from high resolution realisation sub-daily deterministic forecasts of ERA5 is used to cross-check the BLH retrieved from lidar since there is no sounding data in Hefei. The use of "high resolution realization" can be seen from ECMWF website at https://confluence.ecmwf.int/display/CKB/ERA5+data+documentation, the first sentence of third paragraph in the Introduction, "The ERA5 dataset contains one (31 km) high resolution realisation (HRES) and a reduced resolution ten member ensemble (EDA)".

Changes: Page 5, line 22-23. "*The hourly BLH from high resolution realisation sub-daily deterministic forecasts of ERA5 is used to cross-check the BLH retrieved from lidar since there is no sounding data in Hefei.*"

15. For line 18 on page 5, "…… indicated the BLH derived from……", "indicated" should be change to "indicate".

Corrected as suggested.

Changes: Page 6, line 4-5. "*The black dotted line in each panel indicate the BLH derived from RCS, CNR and vertical wind, called as BLH_{RCS}, BLH_{CNR} and BLH_{VAR} in this study.*"

16. For lines 17-19 on page 5, the description could be rewritten as "The black dotted line in each panel indicate the BLH derived from RCS, CNR and vertical wind, called as BLHRCS, BLHCNR and BLHVAR in the study".

Corrected as suggested.

Changes: Page 6, line 4-5. "*The black dotted line in each panel indicate the BLH derived from RCS, CNR and vertical wind, called as BLH_{RCS}, BLH_{CNR} and BLH_{VAR} in this study.*"

17. For Line 24 on page 5: From the author, stratocumulus exists above the ABL; It can be seen clearly from Fig. 3(b) that signals between CBL top and cloud are relatively small, and the BLHs derived by aerosol method are cloud heights. Here, the authors should notice the influence of cloud in BLH retrieving based on lidar.

Thanks for this suggestion. As answered to minor comment 8, the influence of scattered stratocumulus exist in the capping layer with short duration time is negligible in this manuscript. The low level cloud is not exits during this observation. The low level cloud in the ABL can be identified by the paired minimum $W_f(a,b)$ and maximum $W_f(a,b)$ occurs at heights close to each other. The BLH cannot be retrieved under this condition.

Changes: Page 5, line 1-6. "*It should be noted that cloud layer could affect the BLH results. A top-limit is set to the HWCT method for higher clouds. For the scattered stratocumulus that may exist in the capping layer, the differences between cloud top and BLH are relatively small. In addition, the duration time of stratocumulus is also short in the field of view of the lidar. Thus the influence of scattered stratocumulus is negligible. The low level cloud in the ABL can be identified by the paired*

minimum $W_f(a,b)$ and maximum $W_f(a,b)$ occurs at heights close to each other. The BLH cannot be retrieved under this condition."

18. For line 28 on page 5, "The results observed in RCS can be also found in CNR", what is the results? The description is unclear.

We modified this description in revised manuscript. "*The phenomena that observed in RCS described above can be also found in CNR*."

Changes: Page 6, line 16-17. "*The phenomena that observed in RCS described above can be also found in CNR*."

19. For section 4.1, only the observations of aerosol concentration, the resulted ABLH and meteorological parameters are described, so how do they interact with each other? How does the BLH respond to the meteorological condition?

This is a good point. However, it's a complex question that beyond the scope of this manuscript. This paper focuses on the relationship between $PM_{2.5}$ and BLH based on a hybrid lidar in this manuscript. In fact, the meteorological parameters described here are intended to explain the evolution of PM, not the interaction with ABL. These parameters are essential for the study of correlations between BLH and PM concentrations (*Geiß et al.*, 2017). Nevertheless, it seems that there is a strong positive correlation between BLH and temperature. The maximum BLH is lower on 2 June 2018 than that on 1 June 2018, so does the maximum temperature. But this correlation may be due to the cloud-ABL interaction as discussed in Sect. 4.4. A recently accepted work on GRL may be helpful to this question (*Guo et al.*, 2019). The influence of meteorology on the BLH has been investigated using long-term (1979-2016) radiosonde data in this work. More observational and modeling study are needed in future work.

20. For line 25 on page 6, "in Fig. 3, the BLH results are well retrieved, indicating that the HWCT and variance methods are appropriate for BLH determination……" The HWT and variance analysis may be interfered by the RL and cloud layer, how does this study ideal with the interference of them?

Similar to comment 8.

For the HWCT method, we have answered how to deal with cloud layers in response to minor comment 8. An appropriate value of dilation of HWCT may be enough to deal with interference of RL as shown in Fig. R1, and so does an appropriate threshold of variance method as shown in Fig. R2. For the variance method, there is not any interference of cloud layer above the ABL. The low-level cloud that may interfere the results of variance method is not occurred during this observation.

Changes: Page 5, line 1-6. "*It should be noted that cloud layer could affect the BLH results. A top-limit is set to the HWCT method for higher clouds. For the scattered stratocumulus that may exist in the capping layer, the differences between cloud top and BLH are relatively small. In addition, the duration time of stratocumulus is also short in the field of view of the lidar. Thus the influence of scattered stratocumulus is negligible. The low level cloud in the ABL can be identified by the paired*

minimum $W_f(a,b)$ and maximum $W_f(a,b)$ occurs at heights close to each other. The BLH cannot be retrieved under this condition."

21. For line 29 on page 6, "In turbulence derived CBL, all three BLH results from lidar measurements are comparable when the ABL is fully mixed", please improve the description.

We modified this sentence as follows: "*All three retrieved BLH from lidar measurements are comparable when the ABL is fully mixed*."

Changes: Page 7, line 18-19. "*All three retrieved BLH from lidar measurements are comparable when the ABL is fully mixed*."

22. For line 31 on page 6, "a criteria is proposed to classify the ABL as CBL and RL/SBL by the values of BLHVAR and BLHRCS in this study……in the morning, when BLHVAR meets the BLHRCS, the type of ABL changes from RL/SBL into CBL. In the Afternoon, when BLHVAR departs from BLHRCS, the ABL turns into RL/SBL again……." When BLHVAR firstly meets or departs from BLHRCS? How to classify if there are several moments that BLHVAR meets or departs from BLHRCS?

Here we defined $\Delta = BLH_{RCS} - BLH_{VAR}$. There is a hypothesis that BLH_{RCS} (RL) is higher than BLH_{VAR} (SBL) at midnight. This hypothesis is true in most cases. In the morning, the BLH_{VAR} grows with temperature increases. The meet (depart) is defined as when the sign of Δ become negative (positive) for the first (last) time after (before) midnight. If the sign of Δ never changes during the whole day and night, a specified value is used. The meet (depart) is defined as when the value of Δ is less than (greater than) the specified value for the first (last) time after (before) midnight. It should be noted that the specified value varies with different places and seasons. We added more description in the revised manuscript.

Changes: Page 7, line 21-26. "*A parameter is defined as $\Delta = BLH_{RCS} - BLH_{VAR}$. The sign of Δ is positive at nighttime in most cases. In the evening, a SBL is capped by a RL as shown in Fig. 5a. In the morning, when BLH_{VAR} meets the value of BLH_{RCS}, i.e., the sign of Δ become negative or the value of Δ is less than a specified value for the first time after midnight, the type of ABL changes from RL/SBL into CBL. In the Afternoon, when BLH_{VAR} departs from BLH_{RCS}, i.e., the sign of Δ become positive or the value of Δ is greater than a specified value for the last time before midnight, the ABL turns into RL/SBL again.*"

23. For section 4.3, only the "relationship between the BLH and PM2.5" before and after a precipitation case is analyzed. It is not enough to illustrate the title of the manuscripts. In addition, before precipitation, it is clear that the PM shows a contrary tendency with the ABLH. After precipitation, although the ABLH is lower than on previous day maybe caused by cloud or others, the growing process of CBL is similar to that before precipitation, however, there is no obvious tendency of PM2.5. Therefore, what caused the difference of relationship between PM2.5 and ABLH is the PM2.5 distribution. What should be considered is the factor contributing to the difference of PM before and after precipitation, what's role of the precipitation process?

Besides the precipitation, the relationship between BLH and $PM_{2.5}$ is also analyzed with different BLH retrieval methods as shown in Fig. 5d~5e and Table2. A good response of $PM_{2.5}$ to aerosol derived BLH evolution with larger R^2 and stronger correlation than turbulence derived BLH both before and after the precipitation. The correlation between BLH and $PM_{2.5}$ becomes much weaker after the precipitation. The wet growth of existing small particles caused by the precipitation process may be responsible in the early hours. Recently, Geiß et al. (2017) investigated correlations between BLH and concentrations of pollutants (PM_{10}, O_3, NO_x). They found that the correlations of BLH with PM10 were quite different for different sites without showing a clear pattern. The pollution sources, meteorological conditions and details of BLH retrievals should be considered (*Geiß et al.*, 2017). More observational and modeling study are need to solve this question in future work. We added some discussions in the revised manuscript.

Changes:

Page 8, line 23-28. "*The relationships between BLH and PM2.5 are changed after precipitation. Recently, Geiß et al. (2017) investigated correlations between BLH and concentrations of pollutants (PM_{10}, O_3, NO_x). They found that the correlations of BLH with PM_{10} were quite different for different sites without showing a clear pattern. In addition, the reflection and absorption of the incoming solar radiation by the clouds on 2 June 2018 could also affect the diffusion of aerosols. Therefore, BLH with different retrieval methods, pollutant sources and meteorological conditions should be considered in air quality prediction models.*"

Page 9, line 23-24. "*The reasons for the differences in the relationships between BLH and $PM_{2.5}$ may result from both cloud effect and pollutant sources not just the precipitation*."

Page 9, line 26-27. "*To probe the mechanism of the BLH-$PM_{2.5}$ relations under different conditions, such as before and after the precipitation, not only such observations, but also model simulation are needed in further studies.*"

References:

Brooks, I. M., Finding Boundary Layer Top: Application of a Wavelet Covariance Transform to Lidar Backscatter Profiles, Journal of Atmospheric and Oceanic Technology, 20(8), 1092-1105, doi:10.1175/1520-0426(2003)020<1092:fbltao>2.0.co;2, 2003.

Geiß, A., M. Wiegner, B. Bonn, K. Schäfer, R. Forkel, E. von Schneidemesser, C. Münkel, K. L. Chan, and R. Nothard, Mixing layer height as an indicator for urban air quality?, Atmospheric Measurement Techniques, 10(8), 2969-2988, doi:10.5194/amt-10-2969-2017, 2017.

Guo, J., Li, Y., Cohen, J. B., Li, J., Chen, D., Xu, H., Liu, L., Yin, J., Hu, K., Zha, P.: Shift in the temporal trend in boundary layer height trend in China using long-term (1979–2016) radiosonde data, Geophysical Research Letters, doi:10.1029/2019GL082666

Wang, C., Xia, H., Wu, Y., Dong, J., Wei, T., Wang, L., and Dou, X.: Meter-scale spatial-resolution-coherent Doppler wind lidar based on Golay coding, Optics letters, 44, 311-314, 10.1364/OL.44.000311, 2019.

Relationship Analysis of $PM_{2.5}$ and BLH using an Aerosol and Turbulence Detection Lidar

Chong Wang[1,2,*], Mingjiao Jia[2,*], Haiyun Xia[1,2], Yunbin Wu[1], Tianwen Wei[1], Xiang Shang[1], Chengyun Yang[1], Xianghui Xue[1],~~[2],~~ Xiankang Dou[1,3]

[1]CAS Key Laboratory of Geospace Environment, University of Science and Technology of China, Hefei, 230026, China
[2]Glory China ~~Quantum~~Institute of Lidar ~~Co. Ltd.,~~Technology, Shanghai, 201315, China
[3]School of Electronic Information, Wuhan University, Wuhan, 430072, China
[*]These authors contributed equally to this work.

Correspondence to: Haiyun Xia (hsia@ustc.edu.cn)

Abstract. The atmospheric boundary layer height (BLH) is a key parameter in weather forecast and air quality prediction. To investigate the relationship between BLH and air pollution under different conditions, a compact micro-pulse lidar integrated both direct detection lidar (DDL) and coherent Doppler wind lidar (CDWL) is built. ~~Then~~This hybrid lidar is operated at 1.5 μm which is eye-safe and is made of all-fiber components. The BLH can be determined from aerosol density ~~or~~and vertical wind independently. During a 45-hour continuous observation in June 2018, stable boundary layer, residual layer and convective boundary layer are identified. Fine structure of aerosol layers, drizzles and vertical wind near cloudbase are also detected. In comparison, the standard deviation between BLH values derived from DDL and CDWL is ~~60 m~~0. 06 km, indicating the accuracy of this work. The retrieved convective BLH is a little higher than that from ERA5 reanalysis due to different retrieval methods. ~~Negative~~ Correlation between different BLH and $PM_{2.5}$ is ~~analyzed~~strongly negative before ~~and after~~ a precipitation~~. A criterion is proposed to classify~~ event and become much weaker after the ~~residual layer and convective boundary layer.~~precipitation. Different ~~trends show that the relationship~~relations between $PM_{2.5}$ and BLH ~~should be considered in different boundary layer categories~~may result from different BLH retrieval methods, pollutant sources and meteorological conditions.

1 Introduction

In recent decades, with rapid urbanization, air pollution has become a severe environmental problem in China (Chan and Yao, 2008; Li et al., 2016; Song et al., 2017; Zhang et al., 2012). Particulate matter (PM) with aerodynamic diameter less than 2.5 μm ($PM_{2.5}$), attracts public attentions due to its adverse effects on human health and environment (Brunekreef and Holgate, 2002; Cohen et al., 2017; Huang et al., 2014; Kampa and Castanas, 2008). In addition to pollutant emissions and topographic conditions, the spatial and temporal distribution of PM is mainly affected by meteorological conditions in troposphere, especially in atmospheric boundary layer (ABL) (Chen et al., 2018; Li et al., 2017c; Song et al., 2017; Su et al., 2018; Wei et al., 2018).

The ABL, also called PBL (planetary boundary layer), plays an important role in lower troposphere. ABL is directly influenced by and responds to the Earth's surface activities, such as frictional drag, evaporation, transpiration and heat transfer, with a timescale of an hour or less (Stull, 1988). The ABL consists of three major parts during the diurnal evolution: convective boundary layer (CBL), stable boundary layer (SBL) and residual layer (RL) (Stull, 1988). The ABL is a key factor in control and management of air quality, numerical weather prediction, urban and agricultural meteorology, aeronautical meteorology, hydrology and so on (Large et al., 1994). The boundary layer height (BLH) is the height of the top layer of ABL, above which is the free atmosphere. Pollutants or any constituents within this layer is fully mixed and vertically dispersed due to convection or mechanical turbulence (Seibert, 2000). The boundary layer height (BLH) determines the volume available for pollution dispersion and transport in the atmosphere. Low BLH and weak turbulence strengthen the accumulation of air pollutants (Miao et al., 2018; Petaja et al., 2016). Hence, the BLH is one of the fundamental parameters in dispersion models. A roughly anti-correlation relationship between $PM_{2.5}$ and BLH have been found in recent years (Du et al., 2013; Miao et al., 2018; Petaja et al., 2016; Su et al., 2018). However, the relationship analysis of $PM_{2.5}$ and BLH in different ABL categories, i.e., aerosol derived (static) BLH and turbulence derived (dynamical) BLH, is still rare. Therefore, continuous observation of the BLH with high temporal and spatial resolution and the relationship between pollutions and BLH is desirable for air quality prediction.

There are always significant changes in vertical profiles of aerosol concentration, specific humidity, potential temperature or turbulence around the top layer of ABL, making it possible to derive the BLH. There are several instruments used for the determination of BLH based on the sharp gradient in the vertical profiles mentioned above (Baars et al., 2008; Bonin et al., 2018; Li et al., 2017a; Seibert, 2000; Yang et al., 2017). For example, in-situ instruments, such as radiosonde, balloon, mast and aircraft, and remote sensing instruments, such as sodar, wind profiler, lidar and ceilometer. All of these instruments have advantages and shortcomings regarding accuracy, detection range, spatial and temporal resolution as summarized by Seibert (2000). Among these instruments, lidar system provides backscattering signal with sufficient spatial and temporal resolution, long detection range and high accuracy to determine the BLH. These qualities make lidar a powerful tool for BLH assessment. In recent decades, lidars are widely used in lower atmosphere via Mie scattering, Raman scattering and differential absorption (Campbell et al., 2002; Godin et al., 1989; Murray and van der Laan, 1978; Reitebuch, 2012; Renaut et al., 1980; Xia et al., 2007), in middle atmosphere via Rayleigh scattering , in mesosphere and lower thermosphere via fluorescence backscatter . Aerosol, trace gas concentration, atmospheric density and, temperature, and wind, and neutral metal atom can be detected by these lidars. Recently, a micro-pulse direct detection lidar (DDL) based on up-conversion technology was developed to make continuous measurements of aerosol in troposphere (Xia et al., 2015). A coherent detection Doppler wind lidar (CDWL) was developed to measure wind field in ABL (Wang et al., 2017). Different from traditional micro-pulse lidars operated at or near 532 nm (He et al., 2008; Li et al., 2017b; Sawyer and Li, 2013), these two lidars are operated at 1.5 μm, which are eye-safe and can be made with all-fiber components. The 1.5 μm laser shows the highest maximum permissible exposure in the wavelength range from 0.3 to 10 μm (Xia et al., 2015). The invisible infrared eye-safe laser makes these two lidars can work in a densely populated city horizontally. The all-fiber structure makes these lidars robust, immune to external environment changes such as vibration and temperature. Based on these two lidars, BLH values can be derived from both aerosol density

and turbulence. The simultaneous implementation of DDL and CDWL will improve the precision of BLH assessment and enrich the meteorological data in ABL.

Generally, DDL and CDWL belong to different lidar categories. In this work, a hybrid lidar integrating both systems are developed for simultaneous measurements of aerosol and vertical wind. The integrated lidar is utilized to further understand the relationship between $PM_{2.5}$ and BLH. The integrated lidar system, meteorology and PM data are described in Sect. 2. The retrieval methods of BLH are briefly introduced in Sect. 3. In Sect. 4, the results and discussions on lidar data, the retrieved BLH and the relationship between $PM_{2.5}$ and BLH are presented. Finally, the conclusion and summary are drawn in Sect. 5.

2 Instruments and Data

2.1 The integrated lidar system

A compact and integrated micro-pulse lidar system is developed. Benefiting from all-fiber configuration and up-conversion technology, the lidar inherits advantages from both DDL and CDWL. The DDL is based on up-conversion technology and is used for long-range aerosol measurement (Xia et al., 2015). The CDWL is used for wind field measurement (Wang et al., 2017). Two lidar systems use only one set of laser source, optical collimator and control system. The unique optical telescope guarantees that the measured signal in both systems are from the same backscattering volume, and the radial wind profile and aerosol concentration are measured simultaneously.

The diagram of the system is shown in Fig. 1. The seed laser emits continues wave (CW) at 1548 nm, then the CW is split into local oscillator and transmitted seed laser by a beam splitter (BS). The transmitted seed laser is chopped, and frequency shifted 80 MHz by an acoustic-optical modulator (AOM). After the AOM, the transmitted laser is amplified by an Erbium doped fiber amplifier (EDFA) and transmitted into the atmosphere via a collimator. The pulse duration is 300 ns and the pulse energy is 110 μJ. The atmospheric backscattering is collected by two telescopes, adopting double 'D' configuration. As shown in Fig. 1, the two aspheric lenses are glued together with parallel optical axes for easy alignment and avoiding blind zone. The absolute overlap distance is 1 km. On the CDWL channel, the backscattering pass through a circulator is chopped by an optical switch (OS), which cuts off the reflection light from the circulator and lens. The reflection light is much higher than the atmospheric backscattering and will cause saturation and even breakdown in the balanced detector (BD). After the OS, the backscattering is mixed with local oscillator and measured on the BD. The analog signal is converted to digital signal by an ADC and then processed by a PC. On the DDL channel, the backscattering is collected and mixed with a pump laser at 1950 nm in a wavelength division multiplexer (WDM). The mixed laser then passes through the periodically poled lithium niobate waveguide (PPLN). The backscattering at 1548 nm is converted to 863 nm by the PPLN and detected by a Silicon single-photon detector (SPD). A filter is used to filter out the noise. A multi-channel scaler (MCS) records the digital signal. Benefiting from coherent detection and the narrow passband of the PPLN, this integrated lidar can perform all-day detection of the atmosphere. The detailed parameters of the integrated lidar are listed in the Table 1.

During the experiment, the integrated lidar is pointed vertically. Then the vertical wind and backscattering intensity are measured simultaneously. The raw DDL data is recorded with a spatial and temporal interval of 45 m and 2 s, respectively, while CDWL data is 60 m and 2 s, respectively. The integrated lidar is deployed 5 m above ground on the campus of University of Science and Technology of China (USTC, 117.26 °E, 31.84 °N), an urban area in Hefei, China.

2.2 Meteorology and $PM_{2.5}$ data

A weather transmitter (Vaisala WXT520) is used to measure meteorological parameters, including temperature, relative humidity, liquid precipitation, barometric pressure, wind velocity and direction. A visibility sensor (Vaisala PWD50) is used to measure the atmospheric visibility. A wide range aerosol spectrometer (Grimm Mini WRAS 1371) measures aerosol volume size distribution ranging from 10 nm to 35 μm over 41 channels (Shang et al., 2018). Then $PM_{2.5}$ and PM_{10} values are calculated. All these instruments were deployed 60 m above ground and 250 m east of the integrated lidar on the top of a research building in USTC. During the experiment, all these meteorological data are recorded with an interval of 1min.

3 BLH retrieval methods

The BLH is retrieved from both aerosol concentration and vertical wind in this experiment. For the DDL data, the range corrected lidar signal (RCS), $N(R)R^2$, has a sharp decrease at BLH, where $N(R)$ is the backscattering photon number from altitude of R. As for the CDWL, the temporal vertical velocity variation in the ABL is much stronger than that in the free atmosphere. The carrier to noise ratio (CNR) of the CDWL also represents the aerosol concentration, which can also be used to determine the BLH.

Haar wavelet covariance transform (HWCT) method is used to retrieve BLH from aerosol concentration. The HWCT $W_f(a,b)$ is defined as (Brooks, 2003):

$$W_f(a,b) = \frac{1}{a}\int_{z_b}^{z_t} f(z)\, h\left(\frac{z-b}{a}\right) dz \quad , \tag{1}$$

with the Haar function:

$$h\left(\frac{z-b}{a}\right) = \begin{cases} 1, b-\frac{a}{2} \le z \le b \\ -1, b \le z \le b+\frac{a}{2} \\ 0, elsewhere \end{cases} \quad . \tag{2}$$

Where $f(z)$ is the normalized RCS or CNR, z_b and z_t are the bottom and top height of a selected range, a is the dilation of the Haar wavelet and b is the center position of the Haar function. For a given dilation, the height where maximum $W_f(a,b)$ appears is considered to be the BLH. Considering different vertical spatial resolutions and having tested multi values of dilation, a dilation of 150 m and 250 m is applied for RCS and CNR, respectively for this 45-hour observations. Compared with gradient

method, HWCT method has greater adjustability and robustness (Korhonen et al., 2014)~~.~~. The interference by multi aerosol layers in the ABL is negligible for an appropriate dilation. In order to reduce the interference from unexpected ~~turbulence and~~ noise, the signal is averaged to a temporal resolution of 1 min in BLH determination. It should be noted that cloud layer could affect the BLH results. A top-limit is set to the HWCT method for higher clouds. For the scattered stratocumulus that may exist in the capping layer, the differences between cloud top and BLH are relatively small. In addition, the duration time of stratocumulus is also short in the field of view of the lidar. Thus the influence of scattered stratocumulus is negligible. The low level cloud in the ABL can be identified by the paired minimum $W_f(a,b)$ and maximum $W_f(a,b)$ occurs at heights close to each other. The BLH cannot be retrieved under this condition. As described in Sect. 2.1, RCS should be corrected with an overlap factor before the analysis. As an example, the measured RCS and CNR after one-minute average (after overlap correction and background noise deduction) at 1 June 2018, 10:40 am is shown in Fig. 2a. The corresponding HWCT results are shown in Fig. 2b, from which the BLH can be determined.

The BLH can also be determined from the variance of vertical velocity σ_w^2, which ~~represented~~represents the vertical component of the turbulence kinetic energy. For a given time window and a reliable threshold, below the BLH, the σ_w^2 is larger than the threshold, and vice versa. The threshold varies from different locations (Huang et al., 2016). In this study, the threshold is set to be 0.06 m^2s^{-2} which is suitable as shown in Fig. 2c. A median algorithm is used to mitigate the interference and fluctuation from unexpected turbulence and noise~~.~~ in the free atmosphere. Step (1), select all the height with σ_w^2 less than the threshold; Step (2), find the median height z_m selected in Step (1); Step (3), the BLH is the maximum height below z_m that σ_w^2 larger than the threshold. An example of employing this threshold and algorithm is shown in Fig. 2c. Some confusing points, such as that at ~1.0 km and ~1.6 km in Fig. 2c can be distinguished.

~~BLH from~~ Reanalysis data is always used in climatological and regional analysis of BLH (Collaud Coen et al., 2014; Guo et al., 2016; Seidel et al., 2012)~~boundary layer climatology.~~. ERA5 is the newest generation of ECMWF (European Centre for Medium-Range Weather Forecasts) atmospheric reanalysis of the global climate. ERA5 reanalysis assimilates a variety of observations and models in 4-dimensional. The data has 137 levels from the surface up to 80 km altitude, the horizontal resolution is 0.3 °for both longitude and latitude (Hersbach and Dee, 2016). The hourly BLH from high resolution realisation sub-daily deterministic forecasts of ERA5 is used ~~here.~~to cross-check the BLH retrieved from lidar since there is no sounding data in Hefei. The BLH in ERA5 is determined by the bulk Richardson number (Ri_b) method (ECMWF, 2017; Seidel et al., 2012; Vogelezang and Holtslag, 1996). The bulk Richardson number Ri_b is defined as (Vogelezang and Holtslag, 1996):

$$Ri_b = \frac{gh(\theta_{vh} - \theta_{v0})}{\theta_{v0}({u_h}^2 + {v_h}^2)} \quad . \tag{3}$$

Here g is the acceleration of gravity, h is height, θ_{v0} and θ_{vh} are the virtual potential temperature at the surface and h, u_h and v_h are component wind speeds at h, respectively. The BLH is then defined as the lowest height where the Ri_b reaches a critical value of 0.25 (ECMWF, 2017).

Compared to the BLH retrieval, RL top can be identified through a simply rough threshold which is described in the Appendix.

4 Results and discussion

4.1 Observational results

Figure 3 shows a continuous observation over 45 hours from 1 June to 2 June in 2018. The RCS with 1 min temporal resolution, CNR and vertical wind with 20 s temporal resolution are shown, respectively. The black dotted line in each panel ~~indicated~~indicate the BLH derived from RCS, CNR and vertical wind~~. The BLH results are defined~~, called as BLH_{RCS}, BLH_{CNR} and BLH_{VAR} in this study. Meanwhile, the red dotted lines in each panel indicate the RL tops. Sunrise and sunset times at local time (LT) of 05:06 and 19:12 are marked by red triangles and blue inverted triangles. The experimental observation ends with rainfall on the ground at ~2 June, 21:00 LT.

As shown in Fig. 3a, aerosol layer experiences a significant diurnal cycle within a height of 2 km. Before 1 June, 09:00 LT, ~~a~~an aerosol derived SBL caused by radiative cooling from the ground can be easily found below ~0.7 km with higher aerosol concentration than that in the RL. Subsequently, the ABL starts to grow due to solar heating after sunrise and deepens to a maximum height of about 2km in mid-afternoon. Sporadic stratocumulus appears at the top of the ABL with strong backscattering signal. During the night from 1 June, 22:00 to 2 June, 06:00, the backscattering increases in the RL, which is related to the increase of aerosol concentration. After the sunrise on June 2, the ABL grows as it on June 1, but the BLH is lower than that on June 1.

The CNR measured by CDWL is shown in Fig. 3b. The evolution of ABL is similar to that of RCS. The ~~results~~phenomena that observed in RCS described above can be also found in CNR. Figure 3c shows the height-time cross section of vertical wind. To guarantee the precision of the wind measurements, the data with CNR below -35 dB is abandoned (Wang et al., 2017). The downward vertical wind is positive and vice versa. Obviously, the convective ABL is well mixed with strong turbulence during the daytime between sunrise and sunset. Wave-like motions also exist in the nocturnal ABL associated with stratified atmosphere.

Cloud with strong backscattering can be detected between ~3 and ~9 km height by both DDL and CDWL. Corresponding vertical velocity of cloud is measured by the CDWL. Fine cloud structures above the ABL are shown in RCS with high spatial and temporal resolution due to higher detection efficiency. In addition, in the height ranging from ~3 to ~6 km on June 1, several transport aerosol layers can be detected in RCS despite accompanying sunshine induced noise. Interestingly, the transport aerosol layers meet the cloudbase during the night on June 1. The fine structures around cloudbase suggest the existence of drizzles. Moreover, precipitation in cloud can be identified by assuming that precipitation has a fall velocity greater than 1 m s^{-1} (Manninen et al., 2018). A precipitation case is indicated by the red arrow in Fig. 3c at approximately 2 June, 02:00 LT. The $PM_{2.5}$ value measured simultaneously is illustrated as the brown dotted line in Fig. 3c. A sharp increase of $PM_{2.5}$ occurs during the precipitation. These results hint the potential applications of this integrated lidar in the investigations of aerosol-cloud-precipitation interactions.

The simultaneous measurements of meteorological parameters including temperature, pressure, wind velocity, wind direction, visibility and relative humidity near the ground are shown in Fig. 4a to c. It should be noted that the building where the

instrument deployed would have an impact on these meteorological parameters. There is no precipitation event recorded on the ground by weather transmitter, even during the precipitation in the cloud as shown in Fig. 3c. Weak wind condition (velocity less than 4 m s^{-1}) during the whole experiment is not conducive to the aerosol diffusion near the ground. The wind direction is always northly despite the easterly wind before sunrise on June 1. Two haze event occurred, with visibility less than 10 km and relative humidity less than 80%, during this experiment (Administration, 2010). As mentioned before, there is a sudden increase in $PM_{2.5}$ at approximately 2 June, 02:00 LT during the precipitation. There are also sudden changes in relative humidity and visibility at the same time indicated by the vertical dash-dotted lines. Simultaneous measurements of aerosol size volume distribution during this experiment is shown in Fig. 4d. The amount of aerosol rises in all size channels at ~2 June, 02:00 LT. Concentrations of $PM_{2.5}$ and PM_{10} have almost the same evolution processes. It reveals that there is no specified single anthropogenic ~~emissions.~~emission. The wet growth of the existing small particles caused by the precipitation above the ground may be responsible for the sudden increase of aerosols. Therefore, the experiment is chopped into two sections by the precipitation event, as the vertical dash-dotted lines in Fig. 4.

4.2 BLH retrieval results

As shown in Fig. 3, the BLH results are well retrieved, indicating that the HWCT and variance methods are appropriate for BLH determination. A top-limit of 2.5 km of BLH is applied during the BLH retrieval. A comparison is performed as shown in Fig. 5a with retrieved BLH_{RCS}, BLH_{CNR}, BLH_{VAR} and BLH from ERA5 (BLH_{ERA5}). ~~Noted that~~ The BLH_{RCS} and BLH_{CNR} are smoothed with median value by a 5 min temporal window~~.~~ while the BLH_{VAR} is smoothed by a 20 min temporal window. In general, there is a significant diurnal variation in BLH as expected. ~~In turbulence derived CBL,~~ All three retrieved BLH ~~results~~ from lidar measurements are comparable when the ABL is fully mixed. While in nocturnal ABL, the aerosol derived BLH_{RCS} and BLH_{CNR} are much higher than turbulence derived BLH_{VAR} ~~due to residual aerosol and weak turbulence in RL. Therefore, a criteria~~showing the different categories of SBL. A criterion is proposed to classify the ABL as CBL and RL/SBL by the values of BLH_{VAR} and BLH_{RCS} in this study. A parameter is defined as $\Delta = BLH_{RCS} - BLH_{VAR}$. The sign of Δ is positive at nighttime in most cases. In the evening, a SBL is capped by a RL as shown in Fig. 5a. In the morning, when BLH_{VAR} meets the value of BLH_{RCS}, i.e., the sign of Δ become negative or the value of Δ is less than a specified value for the first time after midnight, the type of ABL changes from RL/SBL into CBL. In the Afternoon, when BLH_{VAR} departs from BLH_{RCS}, i.e., the sign of Δ become positive or the value of Δ is greater than a specified value for the last time before midnight, the ABL turns into RL/SBL again. This diurnal evolution of ABL ~~diurnal cycle~~ is similar to that described in Stull (1988) and Collaud Coen et al. (2014). During the RL/SBL, ~~The~~two kinds of SBL ~~and~~ top (RL bottom) are classified by the BLH_{RCS} and BLH_{VAR}. For the CBL, the BLH from lidar is a little higher than BLH_{ERA5}, especially during afternoon. This is in agreement with earlier analysis that climatological BLH based on Richardson's method is substantially lower than BLH derived from other methods (Seidel et al., 2010). While for the turbulence derived SBL, the BLH_{VAR} is comparable with BLH_{ERA5}.

For a quantitative analysis, statistical comparisons of BLH_{RCS} with BLH_{VAR} and BLH_{CNR} are visualized in Fig. 5b and c. The BLH_{VAR} and BLH_{CNR} are plotted versus the corresponding BLH_{RCS}. Scatter diagrams of data points almost lie on the blue and

red dashed lines that represent BLH_{VAR} = BLH_{RCS} and BLH_{CNR} = BLH_{RCS}, respectively. Note that the BLH_{RCS} is interpolated to the same time series of BLH_{VAR} in Fig. 5b and only BLH in CBL is plotted. The BLH_{CNR} agrees well with BLH_{RCS}, despite a difference in RL due to the elevated aerosol layer in the early morning on June 2. The differences between the two results show a standard deviation of 0.06 km of the Gauss fitting. For the CBL, the BLH_{VAR} also agrees well with BLH_{RCS}, with a standard deviation of 0.17 km through Gauss fitting.

4.3 Relationship between $PM_{2.5}$ and BLH

Recently, Su et al. (2018) and Miao et al. (2018) investigated the relationships between the BLH and surface pollutants in China. The influences of topography, seasonal variation, emissions and meteorological conditions on the BLH-$PM_{2.5}$ ~~relationship~~relationships were discussed. Nevertheless, due to the relatively low temporal resolution from space-borne lidar and radiosonde measurements, the influence of different ABL types on the BLH-$PM_{2.5}$ ~~relationship~~relationships are rarely studied.

Figure 5d and e show the relationships between $PM_{2.5}$ concentration and BLH. The correlation coefficients between BLH (BLH_{RCS} in CBL and RL/SBL, and BLH_{VAR} in CBL) and $PM_{2.5}$ before and after precipitation in Fig. 5d and e are listed in Table 2. An obvious anti-correlation is shown before precipitation between BLH and $PM_{2.5}$ concentrations in both CBL and RL/SBL with correlation coefficient of ~ -0.9. An inverse fitting formula $PM_{2.5}=A+B/BLH$ is used to describe the $PM_{2.5}$-BLH relationships in Fig. 5d. The resulted parameters of A, B are listed in Table 2. The nonlinear inverse function shows good performance with coefficient of determination R^2=0.84, 0.65 and 0.85. In general, these results show good responses of $PM_{2.5}$ to aerosol derived BLH (BLH_{RCS}) evolution with larger R^2 and stronger correlation than turbulence derived BLH (BLH_{VAR}) both before and after precipitation. In addition, as shown in Fig. 5d, the inverse function of $PM_{2.5}$ to the BLH_{RCS} and BLH_{VAR} show good consistency in CBL. While in RL/SBL, the inverse function of $PM_{2.5}$ to the BLH_{RCS} is quite different from that in CBL. The parameter A in the inverse fitting formula of the $PM_{2.5}$-BLH relationship for BLH_{RCS} in RL/SBL is triple/twice as large as that for BLH_{RCS}/BLH_{VAR} in CBL as listed in Table 2, while the parameter B has similar values. This difference of parameter A represents a higher $PM_{2.5}$ concentration in RL/SBL. After precipitation, as shown in Fig. 5e and Table 2, there are relatively weak anti-correlations of -0.34, -0.21 and -0.22, respectively. ~~Therefore,~~ The relationships between BLH and PM2.5 are ~~affected by unknown aerosol sources~~ changed after precipitation. Recently, Geiß et al. (2017)~~Therefore,~~ investigated correlations between BLH ~~in~~and concentrations of pollutants (PM_{10}, O_3, NO_x). They found that the correlations of BLH with PM_{10} were quite different ~~ABL categories~~for different sites without showing a clear pattern. In addition, the reflection and absorption of the incoming solar radiation by the clouds on 2 June 2018 could also affect the diffusion of aerosols. Therefore, BLH with different retrieval methods, pollutant sources and ~~weather~~meteorological conditions should be considered in air quality prediction models.

4.4 Aerosol-Cloud-ABL interaction

Moreover, the ABL in cloudy condition on June 2 grows slower with lower BLH than that in fair weather on June 1 as shown in Fig. 5a. The maximum BLH on June 2 is about 1.7 km high while the maximum BLH on June 1 is about 2.3 km high. ~~This~~In addition, the RL tops becomes lower when the cloud layer occurs around 4 km altitude on June 2. These phenomena may be in relation to the aerosol-cloud-ABL interaction. There are several transport aerosol layers above ABL as shown in Fig. 3a. These transport aerosol layers may act as the cloud condensation nuclei during the cloud formation between ~3 and ~5 km on June 2. The clouds play important roles in earth's energy budget. As more incoming solar radiation is reflected and absorbed by clouds, less energy enters the ABL, resulted in weaker CBL development and lower BLH on June 2 than that on June 1. In addition, the weaker convection may lead to the higher aerosol concentration in ABL on June 2 as shown in Fig. 3a and 3(b). These results hinted a strong aerosol-cloud-ABL interaction during the ABL evolution.

5 Conclusion

A compact integrated lidar system that integrates both DDL and CDWL is demonstrated. The DDL incorporated a fiber laser at 1.5 μm and an up-conversion detector. This design of lidar makes it more eye-safe than traditional laser of 355, 532 and 1064 nm. All-fiber configuration is realized to guarantee the high optical coupling efficiency and robust stability. Two lidar systems use only one set of laser source, optical collimator and control system. Thus this integrated lidar can make simultaneous measurements of aerosol density, vertical wind and clouds with high spatial and temporal resolution.

The BLH values derived from aerosol and turbulence are determined from 45-hour continuous measurements. Two methods of HWCT and variance are employed in BLH determination, respectively. ~~The daytime CBL can be recognized by both aerosol and vertical wind measurements. The nocturnal RL can be derived from the aerosol density while nocturnal SBL can be derived from vertical wind measurements.~~The BLH retrieved from different methods are comparable to each other, and so does the RL tops. The standard deviation between aerosol derived BLH from DDL and CDWL is 0.06 km. The BLH derived from vertical wind is comparable with BLH from ERA5 reanalysis data, also with larger BLH than ERA5 due to different retrieval methods as in other studies (Seidel et al., 2010). During the evolution of ABL, the clouds suppress the growth of ABL, leading aerosol increase in ABL. The ~~relationships between~~variations of $PM_{2.5}$ and BLH before and after a precipitation event in clouds are analyzed in different ABL categories adopting different methods ~~are analyzed.~~. There is a strong inverse relation between BLH and $PM_{2.5}$ in both CBL and RL/SBL before a precipitation. However, the relationship is relative weak after the precipitation. In addition, a good response of $PM_{2.5}$ to aerosol derived BLH evolution with larger R^2 and stronger correlation than turbulence derived BLH both before and after the precipitation.

The reasons for the differences in the relationships between BLH and $PM_{2.5}$ ~~under different~~ may result from both cloud effect and pollutant ~~and weather conditions need further studies~~sources not just the precipitation. This required more data based on different instruments, such as horizontal wind field (Shangguan et al., 2017), temperature profiles (Mattis et al., 2002), and depolarization ratio of aerosol (Qiu et al., 2017) ~~in ABL.~~ and pollutant components in ABL. To probe the mechanism of the

BLH-$PM_{2.5}$ relations under different conditions, such as before and after the precipitation, not only such observations, but also model simulation are needed in further studies. The application of such an integrated lidar in this research will contribute to our understanding of ABL and aerosol-cloud-precipitation interactions. Thus improve our ability in weather forecast and air quality prediction in future.

Data availability

The ERA5 data sets are publicly available from ECMWF website at https://www.ecmwf.int/en/forecasts/datasets/reanalysis-datasets/era5, last access, 20 May 2019. Lidar and meteorological data can be downloaded from http://www.lidar.cn/datashare/Wang_et_al_2018c.rar, last access, 20 May 2019.

Appendix: The RL top retrieval method

Besides BLH, RL top is also important in model validation and parameterization development. A simple method to retrieve RL top from RCS, CNR and variance of vertical velocity profiles is proposed. In order to reduce the interference from noise, the RL top is determined with a temporal resolution of 5 min. Dominant aerosol layer tops are easy to be identified around 2 km altitude as shown in Fig, 3. Thus the aerosol layer tops are limited between 1 and 2.5 km altitude range. A threshold method is suitable for RCS and CNR profiles. For this observation, the threshold is set to be 5×10^{10} for RCS profile (1×10^{10} for resolution of 1 min as shown in Fig. 3a) and -30 dB for CNR profile. For profiles of variance of vertical velocity, the aerosol layer is identified as the altitudes under the minimum altitude where invalid data exists, e.g., ~1.6 km in Fig. 2c. If the difference between aerosol layer top and BLH is larger than a threshold, e.g., 0.3 km in current study, the aerosol layer top is identified as RL top. It should be noted that all the values of threshold used here may varies at different places for different lidars. These values may be only suitable for during this observation.

Author contribution

HX and XD conceived and designed the study. CW, YW, TW performed the lidar experiments observations. XS performed the meteorological and PM observations. CY downloaded and analyzed ERA5 data. MJ and CW carried out the data analysis and prepared the figures, with comments from other co-authors. CW, MJ, HX and XX interpreted the data. CW, MJ and HX wrote the manuscript. All authors contributed to discussion and interpretation.

Competing interests.

The authors declare that they have no conflict of interest.

Acknowledgements.

We acknowledge the use of ERA5 data sets from ECMWF website at https://www.ecmwf.int/en/forecasts/datasets/ reanalysis-datasets/era5. We like to thank Dr. Matthias Wiegner for his helpful suggestions. We are grateful to Shengfu Lin, Dr. Mingjia Shangguan and Jiawei Qiu for valuable discussions.

References

Administration, C. M.: Observation and forecasting levels of haze, QX/T 113-2010, China Meteorological Press, Beijing, China, 8, http://www.cma.gov.cn/root7/auto13139/201612/t20161213_350244.html, 2010.

Baars, H., Ansmann, A., Engelmann, R., and Althausen, D.: Continuous monitoring of the boundary-layer top with lidar, Atmospheric Chemistry and Physics, 8, 7281-7296, 10.5194/acp-8-7281-2008, 2008.

Bonin, T. A., Carroll, B. J., Hardesty, R. M., Brewer, W. A., Hajny, K., Salmon, O. E., and Shepson, P. B.: Doppler Lidar Observations of the Mixing Height in Indianapolis Using an Automated Composite Fuzzy Logic Approach, Journal of Atmospheric and Oceanic Technology, 35, 473-490, 10.1175/jtech-d-17-0159.1, 2018.

Brooks, I. M.: Finding Boundary Layer Top: Application of a Wavelet Covariance Transform to Lidar Backscatter Profiles, Journal of Atmospheric and Oceanic Technology, 20, 1092-1105, 10.1175/1520-0426(2003)020<1092:fbltao>2.0.co;2, 2003.

Brunekreef, B., and Holgate, S. T.: Air pollution and health, The Lancet, 360, 1233-1242, 10.1016/s0140-6736(02)11274-8, 2002.

Campbell, J. R., Hlavka, D. L., Welton, E. J., Flynn, C. J., Turner, D. D., Spinhirne, J. D., Scott, V. S., and Hwang, I. H.: Full-Time, Eye-Safe Cloud and Aerosol Lidar Observation at Atmospheric Radiation Measurement Program Sites: Instruments and Data Processing, Journal of Atmospheric and Oceanic Technology, 19, 431-442, 10.1175/1520-0426(2002)019<0431:ftesca>2.0.co;2, 2002.

Chan, C. K., and Yao, X.: Air pollution in mega cities in China, Atmospheric Environment, 42, 1-42, 10.1016/j.atmosenv.2007.09.003, 2008.

Chen, Y., An, J. L., Sun, Y. L., Wang, X. Q., Qu, Y., Zhang, J. W., Wang, Z. F., and Duan, J.: Nocturnal Low-level Winds and Their Impacts on Particulate Matter over the Beijing Area, Advances in Atmospheric Sciences, 35, 1455-1468, 10.1007/s00376-018-8022-9, 2018.

Cohen, A. J., Brauer, M., Burnett, R., Anderson, H. R., Frostad, J., Estep, K., Balakrishnan, K., Brunekreef, B., Dandona, L., Dandona, R., Feigin, V., Freedman, G., Hubbell, B., Jobling, A., Kan, H., Knibbs, L., Liu, Y., Martin, R., Morawska, L., Pope, C. A., Shin, H., Straif, K., Shaddick, G., Thomas, M., van Dingenen, R., van Donkelaar, A., Vos, T., Murray, C. J. L., and Forouzanfar, M. H.: Estimates and 25-year trends of the global burden of disease attributable to ambient air pollution: an analysis of data from the Global Burden of Diseases Study 2015, The Lancet, 389, 1907-1918, 10.1016/s0140-6736(17)30505-6, 2017.

Collaud Coen, M., Praz, C., Haefele, A., Ruffieux, D., Kaufmann, P., and Calpini, B.: Determination and climatology of the planetary boundary layer height above the Swiss plateau by in situ and remote sensing measurements as well as by the COSMO-2 model, Atmospheric Chemistry and Physics, 14, 13205-13221, 10.5194/acp-14-13205-2014, 2014.

Du, C., Liu, S., Yu, X., Li, X., Chen, C., Peng, Y., Dong, Y., Dong, Z., and Wang, F.: Urban Boundary Layer Height Characteristics and Relationship with Particulate Matter Mass Concentrations in Xi'an, Central China, Aerosol and Air Quality Research, 13, 1598-1607, 10.4209/aaqr.2012.10.0274, 2013.

ECMWF: PART IV: PHYSICAL PROCESSES, in: IFS Documentation CY43R3, IFS Documentation, ECMWF, Shinfield Park, Reading, RG2 9AX, England, 221, 2017.

Geiß, A., Wiegner, M., Bonn, B., Schäfer, K., Forkel, R., von Schneidemesser, E., Münkel, C., Chan, K. L., and Nothard, R.: Mixing layer height as an indicator for urban air quality?, Atmospheric Measurement Techniques, 10, 2969-2988, 10.5194/amt-10-2969-2017, 2017.

Godin, S., Mégie, G., and Pelon, J.: Systematic lidar measurements of the stratospheric ozone vertical distribution, Geophysical Research Letters, 16, 547-550, 10.1029/GL016i006p00547, 1989.

Guo, J., Miao, Y., Zhang, Y., Liu, H., Li, Z., Zhang, W., He, J., Lou, M., Yan, Y., Bian, L., and Zhai, P.: The climatology of planetary boundary layer height in China derived from
radiosonde and reanalysis data, Atmospheric Chemistry and Physics, 16, 13309-13319, 10.5194/acp-16-13309-2016, 2016.

He, Q. S., Li, C. C., Mao, J. T., Lau, A. K. H., and Chu, D. A.: Analysis of aerosol vertical distribution and variability in Hong Kong, J Geophys Res-Atmos, 113, Artn D14211
10.1029/2008jd009778, 2008.

Hersbach, H., and Dee, D.: ERA5 reanalysis is in production, Shinfield Park, Reading, Berkshire RG2 9AX, UK, 7, 2016.

Huang, M., Gao, Z., Miao, S., Chen, F., LeMone, M. A., Li, J., Hu, F., and Wang, L.: Estimate of Boundary-Layer Depth Over Beijing, China, Using Doppler Lidar Data During SURF-2015, Boundary-Layer Meteorology, 162, 503-522, 10.1007/s10546-016-0205-2, 2016.

Huang, R. J., Zhang, Y., Bozzetti, C., Ho, K. F., Cao, J. J., Han, Y., Daellenbach, K. R., Slowik, J. G., Platt, S. M., Canonaco, F., Zotter, P., Wolf, R., Pieber, S. M., Bruns, E. A., Crippa, M., Ciarelli, G., Piazzalunga, A., Schwikowski, M., Abbaszade, G., Schnelle-Kreis, J., Zimmermann, R., An, Z., Szidat, S., Baltensperger, U., El Haddad, I., and Prevot, A. S.: High secondary aerosol contribution to particulate pollution during haze events in China, Nature, 514, 218-222, 10.1038/nature13774, 2014.

Kampa, M., and Castanas, E.: Human health effects of air pollution, Environmental pollution, 151, 362-367, 10.1016/j.envpol.2007.06.012, 2008.

Korhonen, K., Giannakaki, E., Mielonen, T., Pfüller, A., Laakso, L., Vakkari, V., Baars, H., Engelmann, R., Beukes, J. P., Van Zyl, P. G., Ramandh, A., Ntsangwane, L., Josipovic, M., Tiitta, P., Fourie, G., Ngwana, I., Chiloane, K., and Komppula, M.: Atmospheric boundary layer top height in South Africa: measurements with lidar and radiosonde compared to three atmospheric models, Atmospheric Chemistry and Physics, 14, 4263-4278, 10.5194/acp-14-4263-2014, 2014.

Large, W. G., Mcwilliams, J. C., and Doney, S. C.: Oceanic Vertical Mixing - a Review and a Model with a Nonlocal Boundary-Layer Parameterization, Reviews of Geophysics, 32, 363-403, Doi 10.1029/94rg01872, 1994.

Li, H., Yang, Y., Hu, X.-M., Huang, Z., Wang, G., Zhang, B., and Zhang, T.: Evaluation of retrieval methods of daytime convective boundary layer height based on lidar data, Journal of Geophysical Research: Atmospheres, 122, 4578-4593, 10.1002/2016jd025620, 2017a.

Li, H., Yang, Y., Hu, X. M., Huang, Z. W., Wang, G. Y., and Zhang, B. D.: Application of Convective Condensation Level Limiter in Convective Boundary Layer Height Retrieval Based on Lidar Data, Atmosphere-Basel, 8, Artn 79 10.3390/Atmos8040079, 2017b.

Li, J., Li, C., Zhao, C., and Su, T.: Changes in surface aerosol extinction trends over China during 1980-2013 inferred from quality-controlled visibility data, Geophysical Research Letters, 43, 8713-8719, 10.1002/2016gl070201, 2016.

Li, Z., Guo, J., Ding, A., Liao, H., Liu, J., Sun, Y., Wang, T., Xue, H., Zhang, H., and Zhu, B.: Aerosol and boundary-layer interactions and impact on air quality, National Science Review, 4, 810-833, 10.1093/nsr/nwx117, 2017c.

Manninen, A. J., Marke, T., Tuononen, M., and O'Connor, E. J.: Atmospheric Boundary Layer Classification With Doppler Lidar, J Geophys Res-Atmos, 123, 8172-8189, 10.1029/2017JD028169, 2018.

Mattis, I., Ansmann, A., Althausen, D., Jaenisch, V., Wandinger, U., Müller, D., Arshinov, Y. F., Bobrovnikov, S. M., and Serikov, I. B.: Relative-humidity profiling in the troposphere with a Raman lidar, Applied optics, 41, 6451, 10.1364/ao.41.006451, 2002.

Miao, Y., Liu, S., Guo, J., Huang, S., Yan, Y., and Lou, M.: Unraveling the relationships between boundary layer height and PM2.5 pollution in China based on four-year radiosonde measurements, Environmental pollution, 243, 1186-1195, 10.1016/j.envpol.2018.09.070, 2018.

Murray, E. R., and van der Laan, J. E.: Remote measurement of ethylene using a CO(2) differential-absorption lidar, Applied optics, 17, 814-817, 10.1364/AO.17.000814, 1978.

Petaja, T., Jarvi, L., Kerminen, V. M., Ding, A. J., Sun, J. N., Nie, W., Kujansuu, J., Virkkula, A., Yang, X. Q., Fu, C. B., Zilitinkevich, S., and Kulmala, M.: Enhanced air pollution via aerosol-boundary layer feedback in China, Scientific reports, 6, 6, 10.1038/srep18998, 2016.

Qiu, J., Xia, H., Shangguan, M., Dou, X., Li, M., Wang, C., Shang, X., Lin, S., and Liu, J.: Micro-pulse polarization lidar at 1.5 mum using a single superconducting nanowire single-photon detector, Optics letters, 42, 4454-4457, 10.1364/OL.42.004454, 2017.

Reitebuch, O.: Wind Lidar for Atmospheric Research, in: Atmospheric Physics, edited by: Schumann, U., Research Topics in Aerospace, Springer, Berlin, Heidelberg, 487-507, 2012.

Renaut, D., Pourny, J. C., and Capitini, R.: Daytime Raman-lidar measurements of water vapor, Optics letters, 5, 233-235, 10.1364/ol.5.000233, 1980.

Sawyer, V., and Li, Z.: Detection, variations and intercomparison of the planetary boundary layer depth from radiosonde, lidar and infrared spectrometer, Atmospheric Environment, 79, 518-528, 10.1016/j.atmosenv.2013.07.019, 2013.

Seibert, P.: Review and intercomparison of operational methods for the determination of the mixing height, Atmospheric Environment, 34, 1001-1027, 10.1016/s1352-2310(99)00349-0, 2000.

Seidel, D. J., Ao, C. O., and Li, K.: Estimating climatological planetary boundary layer heights from radiosonde observations: Comparison of methods and uncertainty analysis, J Geophys Res-Atmos, 115, 10.1029/2009jd013680, 2010.

Seidel, D. J., Zhang, Y. H., Beljaars, A., Golaz, J. C., Jacobson, A. R., and Medeiros, B.: Climatology of the planetary boundary layer over the continental United States and Europe, J Geophys Res-Atmos, 117, 10.1029/2012jd018143, 2012.

Shang, X., Xia, H., Dou, X., Shangguan, M., Li, M., and Wang, C.: Adaptive inversion algorithm for1.5 μm visibility lidar incorporating in situ Angstrom wavelength exponent, Optics Communications, 418, 129-134, 10.1016/j.optcom.2018.03.009, 2018.

Shangguan, M., Xia, H., Wang, C., Qiu, J., Lin, S., Dou, X., Zhang, Q., and Pan, J. W.: Dual-frequency Doppler lidar for wind detection with a superconducting nanowire single-photon detector, Optics letters, 42, 3541-3544, 10.1364/OL.42.003541, 2017.

Song, C., Wu, L., Xie, Y., He, J., Chen, X., Wang, T., Lin, Y., Jin, T., Wang, A., Liu, Y., Dai, Q., Liu, B., Wang, Y. N., and Mao, H.: Air pollution in China: Status and spatiotemporal variations, Environmental pollution, 227, 334-347, 10.1016/j.envpol.2017.04.075, 2017.

Stull, R. B.: An Introduction to Boundary Layer Meteorology, Kluwer Academic Publishers., Dordrecht. The Netherlands., 1988.

Su, T., Li, Z., and Kahn, R.: Relationships between the planetary boundary layer height and surface pollutants derived from lidar observations over China: regional pattern and influencing factors, Atmospheric Chemistry and Physics, 18, 15921-15935, 10.5194/acp-18-15921-2018, 2018.

Vogelezang, D. H. P., and Holtslag, A. A. M.: Evaluation and model impacts of alternative boundary-layer height formulations, Boundary-Layer Meteorology, 81, 245-269, 10.1007/bf02430331, 1996.

Wang, C., Xia, H., Shangguan, M., Wu, Y., Wang, L., Zhao, L., Qiu, J., and Zhang, R.: 1.5 μm polarization coherent lidar incorporating time-division multiplexing, Optics express, 25, 20663-20674, 10.1364/OE.25.020663, 2017.

Wei, W., Zhang, H., Wu, B., Huang, Y., Cai, X., Song, Y., and Li, J.: Intermittent turbulence contributes to vertical dispersion of $PM_{2.5}$ in the North China Plain: cases from Tianjin, Atmospheric Chemistry and Physics, 18, 12953-12967, 10.5194/acp-18-12953-2018, 2018.

Xia, H., Sun, D., Yang, Y., Shen, F., Dong, J., and Kobayashi, T.: Fabry-Perot interferometer based Mie Doppler lidar for low tropospheric wind observation, Applied optics, 46, 7120, 10.1364/ao.46.007120, 2007.

Xia, H., Shentu, G., Shangguan, M., Xia, X., Jia, X., Wang, C., Zhang, J., Pelc, J. S., Fejer, M. M., Zhang, Q., Dou, X., and Pan, J. W.: Long-range micro-pulse aerosol lidar at 1.5 μm with an upconversion single-photon detector, Optics letters, 40, 1579-1582, 10.1364/OL.40.001579, 2015.

Yang, T., Wang, Z., Zhang, W., Gbaguidi, A., Sugimoto, N., Wang, X., Matsui, I., and Sun, Y.: Technical note: Boundary layer height determination from lidar for improving air pollution episode modeling: development of new algorithm and evaluation, Atmospheric Chemistry and Physics, 17, 6215-6225, 10.5194/acp-17-6215-2017, 2017.

Zhang, Q., He, K., and Huo, H.: Policy: Cleaning China's air, Nature, 484, 161-162, 10.1038/484161a, 2012.

Table 1. Key Parameters of the Integrated Lidar.

Parameter	CDL	DDL
Wavelength	1548 nm	
Pulse Duration	300 ns	
Pulse Energy	110 μJ	
Repetition frequency	10 kHz	
Diameter of collimator	80 mm	
Diameter of telescope	80 mm	70 mm
Spatial resolution	45 m	
Temporal resolution	2 s	
Maximum range	15 km	
Azimuth scanning range	0 - 360 °	
Zenith scanning range	0 - 90 °	

Table 2. The correlations between BLH and $PM_{2.5}$ and the inverse fitting results.

Time	Before precipitation			After precipitation		
ABL	CBL	CBL	RL/SBL	CBL	CBL	RL/SBL
BLH	BLH_{RCS}	BLH_{VAR}	BLH_{RCS}	BLH_{RCS}	BLH_{VAR}	BLH_{RCS}
C[a]	-0.92	-0.89	-0.93	-0.34	-0.21	-0.22
A[b]	7.98	12.46	23.16			
B[b]	42.22	35.92	32.65			
R^2 [c]	0.84	0.65	0.85			

[a] C: Correlation coefficients.

[b] A/B: The parameters of the inverse fitting formula $PM_{2.5}=A+B/BLH$.

[c] R^2: Coefficient of determination of the inverse fitting.

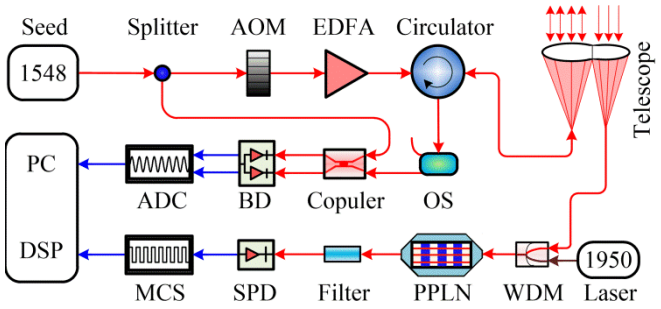

Figure 3: The diagram of the integrated lidar system.

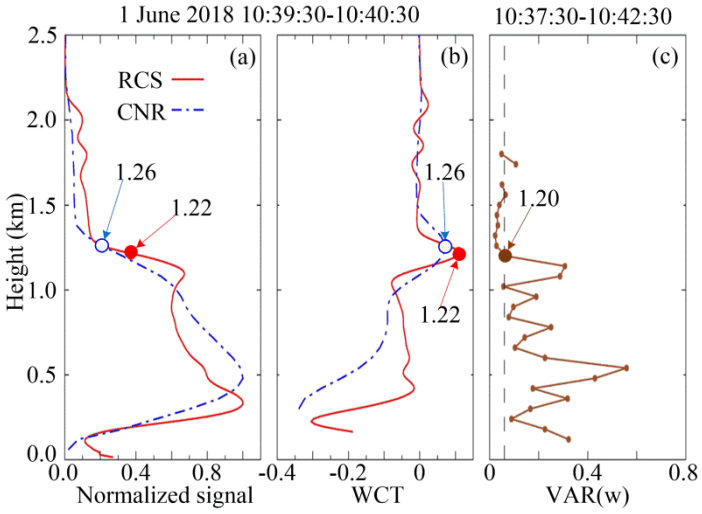

Figure 2: (a) 1 min mean normalized RCS and CNR profiles. (b) The corresponding HWCT results of the RCS and CNR profiles in (a). (c) The vertical velocity variance profile. The black dashed line indicated the threshold of 0.06 m^2s^{-2}. The red solid circle, blue circle and brown solid circle denoted by the arrows indicate the retrieved BLH, with the values at the end of the arrows.

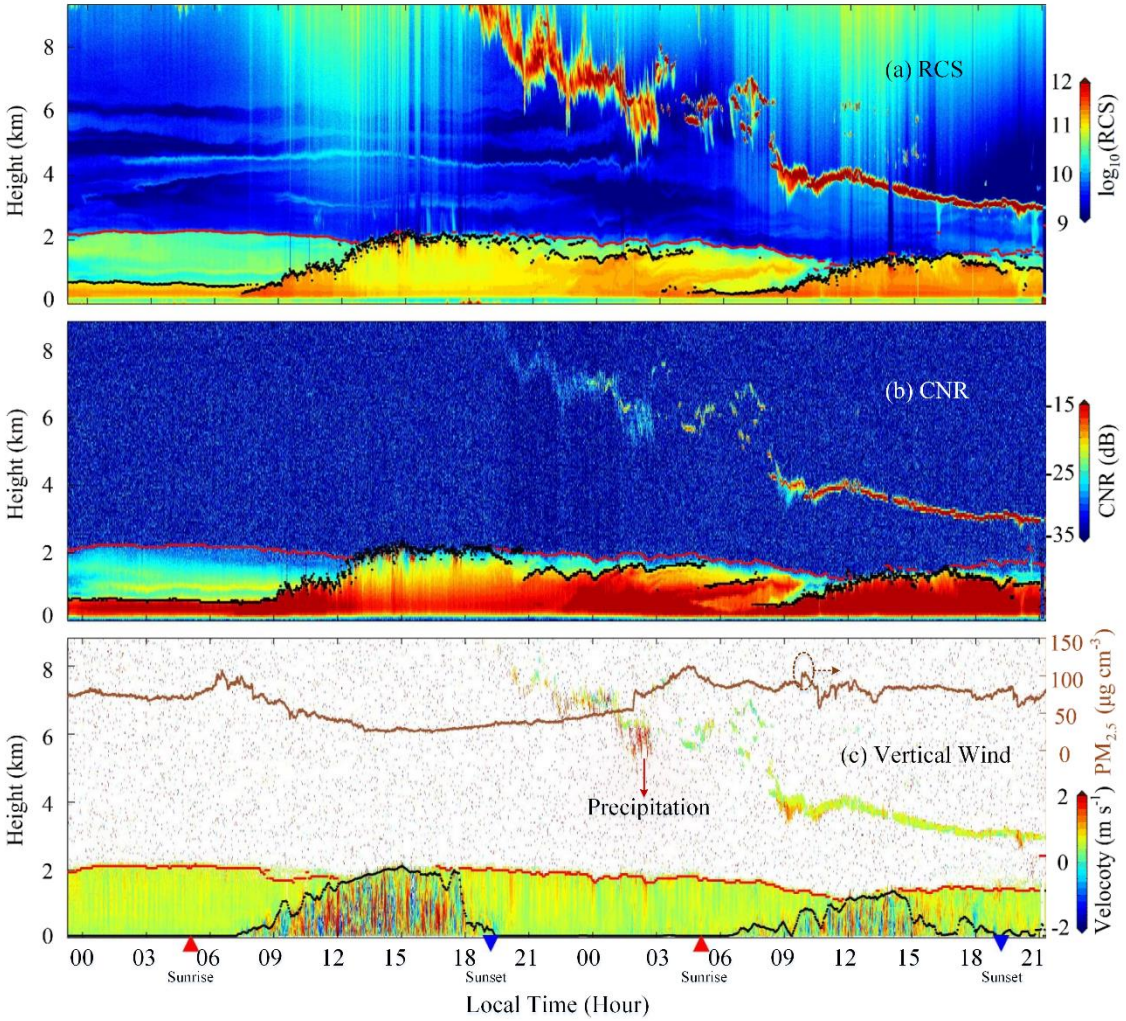

Figure 3: Lidar observational results from 1 June 2018 to 2 June 2018. (a) The 1 min mean time series of logarithmic RCS profiles measured by DDL. The height time cross section of (b) CNR and (c) vertical wind measured by CDWL with 20 s temporal interval. The downward (upward) vertical wind is positive (negative). The brown dotted line indicates the $PM_{2.5}$ concentration near the ground. The black (red) dotted lines in each panel indicates the BLH (RL tops) retrieved from RCS, CNR and vertical wind, respectively.

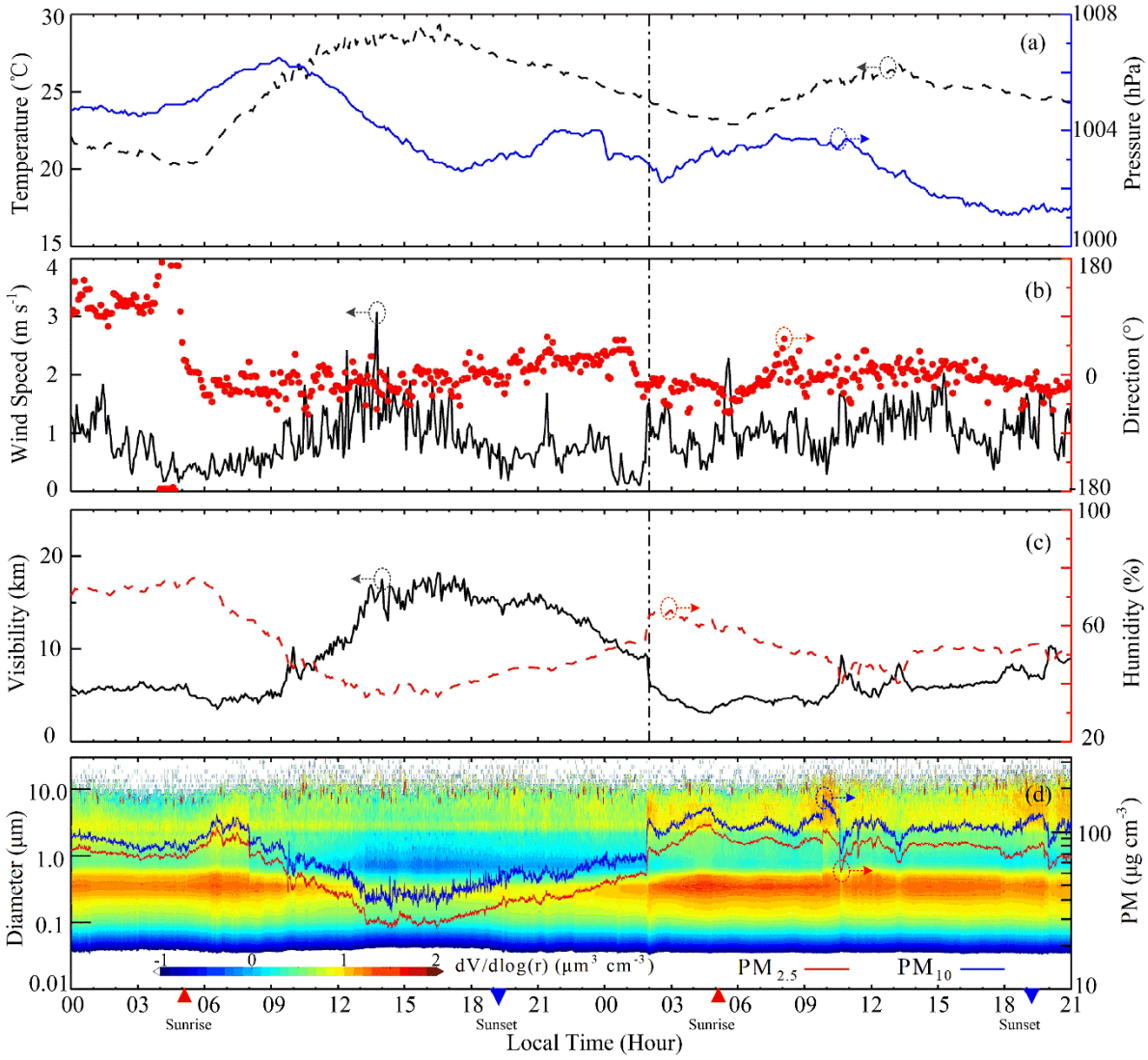

Figure 4: The simultaneous measured surface meteorological parameters during the experiment from 1 June 2018 to 2 June 2018. From top panel to bottom panel are (a) temperature, pressure; (b) wind velocity, wind direction; (c) visibility, relative humidity; (d) logarithmic aerosol volume size, PM2.5 and PM10 concentration, respectively. The vertical dashed lines in (a)-(c) indicate the time when there is a sudden enhancement of $PM_{2.5}$ in (d).

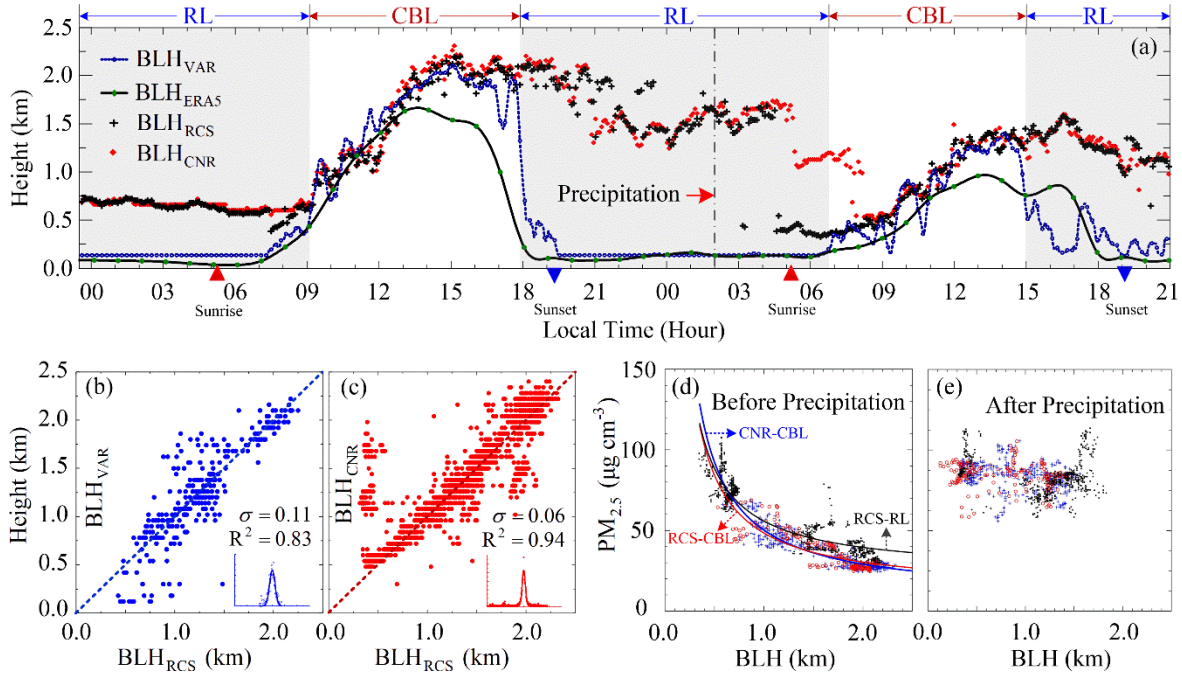

Figure 5: (a) The BLH retrieval results from different methods. Scatter plots of (b) BLH_{VAR} in CBL and (c) BLH_{CNR} in CBL and RL versus BLH_{RCS} for comparison. The blue and red dashed lines indicate x = y. The BLH differences are plotted in right bottom in (b) and (c). The blue and red solid lines represent the corresponding Gauss fitting. R^2 represents the coefficient of determination and σ represents the standard deviation of Gauss fitting. (d) The scatter plot of BLH and PM2.5 before precipitation. Red circles indicate BLH_{VAR} in CBL, while blue pluses indicate BLH_{RCS} in CBL and black dots indicate BLH_{RCS} in RL. The solid lines represent the corresponding inverse fit. (e) Same as (d) but without inverse fitting after precipitation.